VISCOELASTIC ANALYSIS OF SANDWICH BEAMS HAVING ALUMINUM AND FIBER-REINFORCED POLYMER SKINS WITH A POLYSTYRENE FOAM CORE

A Thesis

by

ALTRAMESE LASHÉ ROBERTS-TOMPKINS

Submitted to the Office of Graduate Studies of
Texas A&M University
in partial fulfillment of the requirements for the degree of

MASTER OF SCIENCE

December 2009

Major Subject: Mechanical Engineering

VISCOELASTIC ANALYSIS OF SANDWICH BEAMS HAVING ALUMINUM AND FIBER-REINFORCED POLYMER SKINS WITH A POLYSTYRENE FOAM CORE

A Thesis

by

ALTRAMESE LASHÉ ROBERTS-TOMPKINS

Submitted to the Office of Graduate Studies of
Texas A&M University
in partial fulfillment of the requirements for the degree of

MASTER OF SCIENCE

Approved by:

Chair of Committee,	Anastasia Muliana
Committee Members,	Hong Liang
	Karen Butler-Purry
Head of Department,	Dennis O'Neal

December 2009

Major Subject: Mechanical Engineering

ABSTRACT

Viscoelastic Analysis of Sandwich Beams Having Aluminum and Fiber-Reinforced Polymer Skins with a Polystyrene Foam Core. (December 2009)

Altramese LaShé Roberts-Tompkins, B.S., University of Detroit Mercy

Chair of Advisory Committee: Dr. Anastasia Muliana

Sandwich beams are composite systems having high stiffness-to-weight and strength-to-weight ratios and are used as light weight load bearing components. The use of thin, strong skin sheets adhered to thicker, lightweight core materials has allowed industry to build strong, stiff, light, and durable structures. Due to the use of viscoelastic polymer constituents, sandwich beams can exhibit time-dependent behavior. This study examines and predicts the time-dependent behavior of sandwich beams driven by the viscoelastic foam core. Governing equations of the deformation of viscoelastic materials are often represented in differential form or hereditary integral form. A single integral constitutive equation is used to model linear viscoelastic materials by means of the Boltzmann superposition principle. Based on the strength of materials approach, the analytical solution for the deformation in a viscoelastic sandwich beam is determined based on the application of the Correspondence Principle and Laplace transform. Finite element (FE) method is used to analyze the overall transient responses of the sandwich systems subject to a concentrated point load at the midspan of the beam. A 2D plane strain element is used to generate meshes of the three-point bending beam. User material

(UMAT) subroutine in ABAQUS FE code is utilized to incorporate the viscoelastic constitutive model for the foam core. Analytical models and experimental data available in the literature are used to verify the results obtained from the FE analysis. The stress, strain, and deformation fields during creep responses are analyzed. Parameters such as the viscosity of the foam core, the ratio of the skin and core thicknesses, the ratio of the skin and core moduli, and adhesive layers are varied and their effect on the time-dependent behavior of the sandwich system is examined.

DEDICATION

To my loving husband, family, and friends for their prayers, love, patience, and support

ACKNOWLEDGEMENTS

I would like to thank my research advisor, Dr. Anastasia Muliana for her guidance, support, and patience. She was a mentor and encourager, always providing her expertise and knowledge. I want to thank her for believing in me and helping me through challenging times. I would like to extend my appreciation to my committee members, Dr. Hong Liang, Dr. Nicole Zacharia, Dr. Karen Butler-Purry for their supporting roles in this process. Dr. Liang, I thank you for being patient and supportive. Dr. Butler-Purry, I thank you for being patient and always offering to provide help, guidance, and advice. Dr. Zacharia, I thank you for stepping in to provide your support and time to help in the completion of my degree. Thanks also go to the faculty and staff in the Department of Mechanical Engineering and Office of Graduate Studies at Texas A&M University that helped me through this journey.

I would like to thank God for keeping me and showing me through him all things are possible. I want to thank my loving husband for being my rock and my best friend. I truly admire his commitment to not only me, but also his perseverance on his journey to earning a PhD. I want to thank my parents, who have encouraged me to always do my best, never give up, and to always remain humble. They have always provided love, wisdom, and faith. Thank you to my wonderful sister and brother-in-law, for your encouragement and love. Grandma Ola, I admire you for your strength and leadership. I thank you for your encouragement, love, and for being a strong woman role model that I

can always look up to. To all my family (aunts, uncles, cousins, and in-laws), friends, and church family thank you for your support and encouragement.

Thank you God for blessing me with the time I had as a granddaughter, niece, and cousin to Grandpa and Grandma Griffin, Aunt Jacquline, Aunt Sarah, and Dezireh for they will all be truly missed and I love them very much.

TABLE OF CONTENTS

CHAPTER Page

LIST OF FIGURES

FIGURE Page

FIGURE Page

FIGURE Page

LIST OF TABLES

CHAPTER I

INTRODUCTION

Sandwich beams are composite systems having low weight and high strength- and stiffness characteristics. Typical sandwich beams consist of two thin skin layers separated by a thick inner core. The use of thin, strong skin sheets adhered to thicker, lightweight core materials has allowed industry to build strong, stiff, light, and durable structures. When the skins and core are joined together, they function as a single structural component containing all the advantages of each component. Sandwich beams have high stiffness-to-weight and strength-to-weight ratios and are used as light weight load bearing components. Tensile and compressive stresses are mainly carried by the skins, while transverse shear stresses are predominantly experienced by the core. Typically, materials such as steel and aluminum sheets are used for the skins, but fiber-reinforced polymers (FRP) are prevalent. The main function of the core is to increase the flexural rigidity of the sandwich beam, minimizing transverse deformation. Honeycombs, foams, and corrugated cores made of polymers or metals are typically used.

Historically, the first use of the concept of sandwich construction dates back to Sir William Fairbairn in England 1849. The idea to combine two different materials to increase the strength of a structure was first used in the 1930s. In 1940, sandwich

---

This thesis follows the style of International Journal of Solids and Structures.

construction was used extensively in building the English Mosquito bomber during the War II. The Mosquito was implemented with a plywood sandwich construction. In the United States the core was originated. In the late 1940's, Hexcel Corporation was formed and it has played the most role in the development of sandwich construction. Sandwich beams are widely used in a variety of applications such as satellites, railroads, and automobiles to name a few (Vinson, 2005).

Due to the use of polymer constituents, sandwich beams can exhibit time-dependent behavior. Viscoelasticity is the study of time-dependent materials showing a combined elastic solid and viscous fluid behavior when subjected to external mechanical loadings. The response of viscoelastic materials is determined not only by the current state of the load, but also by the history of the loading (Wineman and Rajagopal, 2000).

This chapter presents a literature review of analytical, numerical, and experimental works on viscoelastic behaviors of sandwich beams having metal and FRP skins and polymer foam cores. The research objectives of the present study will be discussed.

1.1 STATE OF THE ART KNOWLEDGE IN VISCOELASTIC SANDWICH BEAMS

1.1.1 VISCOELASTIC BEHAVIORS OF SANDWICH BEAMS WITH METAL OR FRP SKINS AND POLYMER FOAM CORES

Polymer foam cores are being used in load-bearing applications (e.g. sandwich beams). When dealing with sandwich polymer foam cores, understanding their

viscoelastic behaviors (e.g. creep, relaxation) become essential. The mechanical behavior of a viscoelastic material can be expressed in terms of extension, shear, and bulk moduli compliances respectively (Theocaris, 1964). Huang and Gibson (1990) discussed modeling creep responses of sandwich beams having linear viscoelastic polymer foam cores. Total deflections in a sandwich beam subject to transverse loads are determined by combining the effects of bending moment and transverse shear force. The bending component of the deflection of a sandwich beam with elastic skins and viscoelastic core show insignificant time-dependent response, due to the stiff elastic skins while the shearing component shows a significant increase in deformation with time.

Huang and Gibson (1990) tested sandwich beams made of aluminum skins bonded to polyurethane foam cores. They fabricated sixteen beams having core densities; 32, 48, 64, 96 kg/m^3. All the beams were loaded under three-point bending with constant dead weights in a temperature controlled chamber for 1200 hours. The mid-point deflection was measured using linear variable transducers (LVDTs) or dial gages. The measurements were taken at fixed time intervals throughout the loading phase and for 450 hours after unloading. Huang and Gibson (1990) concluded that the analytical model obtained from the strength of material approach gave a good depiction of the creep deformation of the sandwich beams. Huang and Gibson (1990) showed that long-term creep can be calculated by extrapolating short-term results for any density foam core, under any load, provided the foam is linear viscoelastic.

Kim and Swanson (2001) performed experimental tests on sandwich beams with carbon/epoxy skins and high-density rigid polyurethane foam cores. The skins and cores were supplied in three different thicknesses and densities respectively. Kim and Swanson (2001) used several analytical models to determine the stresses and deformations from three-point bending tests and they are: (1) the classical strength of material theory, which assumes plane sections remain plane and normal to the centerline, (2) the first-order shear deformation theory in which plane sections are assumed to remain plane, but are not normal to the centerline due to shear angles, (3) the elasticity theory which is an exact three dimensional (3D) solution to the problem of transverse loading of a layered solid with simply-supported boundary conditions, (4) the higher order theory that treats each skin as an independent beam and an approximate solution is developed for the core, and (5) the two dimensional (2D), finite element (FE) solution using ANSYS. Responses from the above analytical models were compared with experimental data. The elasticity and FE methods were shown to be comparable. In the analytical methods used by Kim and Swanson (2001), the classical theory was found to over-predict the stiffness of sandwich beams, while the first-order shear deformation theory and the higher order beam theory gave acceptable results for stiffness. The first-order shear deformation theory and classical theory are not capable of predicting localized strains and stresses near the applied concentrated load.

1.1.2 ANALYTICAL PREDICTION OF THE CREEP EFFECT ON SANDWICH BEAMS USING LINEAR VISCOELASTIC MODELS

Shenoi et al. (1997) studied the long-term effects of creep as well as creep fatigue, for the sandwich beams having FRP skins and a polyvinyl chloride (PVC) foam core. If a material is tested within the range of linear responses, simple rheological models can be used to describe the viscous and elastic behavior. These models are developed using combinations of mechanical components such as dashpots, i.e., linear viscous elements, and springs, i.e., linear elastic elements which are used to construct Maxwell and Kelvin-Voigt (Voigt) models (Nuñez et al., 2004; Qiao et al., 2000). Shenoi et al. (1997) and Nuñez et al. (2004) modeled creep using the linear viscoelastic Burgers model and the time-dependent responses are compared to experimental results. The Burgers model consists of a Maxwell model (i.e. a spring and dashpot in series) and Kelvin-Voigt model (i.e. a spring and dashpot in parallel) connected in series as the simplest model used that displays instantaneous elastic, time-dependent (i.e. transient), and permanent deformations. It is assumed that there is a linear correlation between the stress and time dependent strain. The Burgers model was reported to give a satisfactory representation of linear viscoelastic behavior (Nuñez et al., 2004).

The study performed by Gnip et al. (2005a, b) focused on the phenomenological model of creep strain in expanded polystyrene (EPS) in terms of nonlinear viscoelasticity. Creep responses can be described using power law and exponential functions. In Gnip et al. (2005a), expanded polystyrene plates under constant stress were tested, varying the density and EPS grades. Long-term test were carried out for various

durations, i.e., in days at a constant stress. Gnip et al. (2005b) discussed predicting long-term deformation using extrapolation, which is a regression analysis method used for prediction. Specifically, the extrapolation was used to forecast time-series data. Extrapolation makes is possible to construct long-term deformation for certain duration provided the correct model was chosen. New data points are constructed based on a discrete set of known data points, which in the case would be experimental data. Short-term creep test results within a period of 65 to 608 days were analyzed by Gnip et al. (2005b) and extrapolated to predict creep for 50 years. By using statistical means, i.e. least squares, root-mean-square deviations, squared correlation ratio, and regression equations the experiments performed in Gnip et al. (2005a, b) showed that creep curves and strains could be predicted accurately by the power law. Nuñez et al. (2004) demonstrated the possibility of long-term creep data being predicted from short-term test data of different isothermal conditions if the time-temperature superposition was applicable by creating master curves that can be constructed to obtain long-term data in conditions where aging could be neglected.

In the past four decades, many papers have been published on analytical and experimental methods describing the long-term behavior of FRP composites (Scott et al., 1995). Time-dependent behavior of FRP composites can be greatly influenced by parameters such as environmental conditions, mechanical loads, or a combination of both. A wide range of analytical models have been developed to predict the time-dependent behavior of polymers. The main macro-mechanical theories used in viscoelastic theory stated by Scott et al. (1995) are: the Findley power law model, rule of

mixtures approach for combining the effects of the time-dependent behavior of the matrix and reinforcing materials to describe the viscoelastic behavior of the composite structure, Schapery single integral procedure, and the Boltzmann superposition principle. Findley's power law is extensively used in analytical models describing viscoelastic behavior of FRP composites under constant stress. Scott et al. (1995) stated that the Boltzmann superposition principle works for linear viscoelastic material and is no longer applicable for a nonlinear viscoelastic material unless modifications, such as the inclusivity of factors that are functions of stress and temperature, i.e., Schapery integral are made to account for nonlinear behavior.

1.1.3 DESIGN AND OPTIMIZATION FOR SANDWICH BEAMS

Sandwich beams are generally thick structures in which the thickness is not negligible as compared to other dimensions. Thus, shear deformation accounts for a significant amount of transverse deflection (Hartsock, 1969). In polymer foam cores, shear deformation often continues to increase under a constant load (stress). The strength of a sandwich beam is determined by the resistance of the skins or core to failures. Ideally, the skins should be designed to resist axial stresses, whereas the core should be designed for limited shear. Although the distribution of the shear stress through the thickness in sandwich beams is not uniform, for design purposes the shear stress through the core thickness is often assumed uniform. Hartsock (1969) found urethane foam to behave well under short-term loads, but under long-term loads the deflection continued to increase leading to instability in the structure. Swanson and Kim (2002) show that the

first order shear deformation theory (FSDT) is not adequate to capture deformation in the sandwich beams. The FSDT is not suitable to predict deformation, stress, and strain because one of the key assumptions that the plain section remains straight after deformation is violated. Swanson and Kim (2002) mentioned that the elasticity theory provided good accuracy when compared to FE analyses in previous work, and with surface and embedded strain gages, which is suitable for repetitive calculations. The elasticity theory was reviewed and compared with experimental data for strain distributions.

Steeves and Fleck (2004) presented several possible failure modes in sandwich beams. The active mode is based on beam geometry, material properties, and loading configurations. Failure modes for core shear failure, delamination, and shear and compression failures were examined in Swanson and Kim (2002), Steeves and Fleck (2004). Lim et al. (2004) and Sharma and Raghupathy (2008) also listed several failure modes for foam core sandwich beams under bending which are skin fracture, skin wrinkling, core shear yield, core compressive yield, and interfacial failure between the core and the skins. Failure can also occur due to the debonding of adhesive in the sandwich beam. Listed below are detailed descriptions of how these failures occur (Lukkassen and Meidell, 2007):

1. Skin yielding or fracture of the skin occurs when the normal stress in the skins is equal to or greater than the yield strength of the skin material
2. Skin wrinkling or local buckling occurs when the normal stress in the skin attains the local stress and is influenced most by the core

3. Core shear failure occurs when the shear stress is equal to or greater than the yield strength of the core in shear
4. Failure of adhesive bond between the skins and core occurs dues to high thermal stresses, fatigue, and aging
5. General buckling occurs due to transverse shear deformation
6. Skin dimpling or local buckling occurs in sandwich beams with honeycomb or corrugated core materials
7. Fatigue occurs when a sandwich beam's fatigue limit or maximum allowable stress is exceeded and damage is experienced. The failure mode is the cause of failure by most structures.

Failure modes are analyzed and used to determine the design limits on sandwich beams. Ductile metallic skins naturally exhibit yielding behavior, while FRP skins tend to be more brittle (Swanson and Kim, 2002). In Swanson and Kim (2002) carbon/epoxy laminated skins were considered in experiments in which the strain was shown to be an accurate failure criterion. A detailed procedure can be used to obtain optimum ratios for skin to core weight along with core density and thickness, to optimize the strength to weight ratio (Hartsock, 1969). Optimum designs for strength in sandwich beams under concentrated loads appeared to select high density cores (Swanson and Kim, 2002).

1.2 RESEARCH OBJECTIVES

The objective of this study is to perform parametric studies to examine and predict the time-dependent behavior of sandwich beams under three-point bending

driven by the viscoelastic foam core. Based on the strength of materials approach, an analytical solution for deformation in linear elastic sandwich beams is determined and the Correspondence Principle is employed to obtain solutions for deformations in linear viscoelastic sandwich beams. The Correspondence Principle provides the means to convert the linear elastic solutions into solutions for linear viscoelastic problems. There are conditions where the Correspondence Principle is not applicable. In order to apply the Laplace transform; the displacement must be defined at all times for $t \geq 0$, the motion of the viscoelastic body must be quasi-static, and at a fixed point on the boundary, the prescribed boundary condition cannot be changed from one specifying displacement to one specifying surface traction during and vice versa (Wineman and Rajagopal, 2000). Solutions to linear viscoelastic problems can be obtained directly from the corresponding linear elastic solutions through the use of the Laplace transform (Wineman and Rajagopal, 2000). Material parameters in the linear elastic solutions are replaced by a product of Laplace transformed variables of solutions to viscoelastic problems. The solutions are transformed back to the time domain solutions. Analytical results show minimal deviation from available experimental data.

In addition, the FE method is also used to perform parametric studies. Parameters such as the viscosity of the foam core, the ratio of the skin and core thicknesses, the ratio of the skin and core moduli, and adhesive layers will be varied and the effects of these parameters on the time-dependent behavior of sandwich beams are examined. Understanding the time-dependent deformation will be of great importance in predicting long-term behavior of polymer foam core sandwich beams. The numerical analysis for

the research is done using ABAQUS FE. Models of the sandwich beams are generated using 2D continuum elements.

Chapter II depicts the analytical solution for deformation in viscoelastic sandwich beams subject to three-point bending. Constitutive models for linear isotropic viscoelasticity are derived from linear combinations of springs and dashpots representing the elastic and viscous components in viscoelastic behavior. Common models used to predict the response of viscoelastic materials, i.e., the Maxwell model, the Kelvin-Voigt model, the Standard Linear Solid (SLS) model, and the Burgers model are discussed. The characteristic creep and relaxation times is the time at which considerable stress relaxation or creep has occurred in a step test (Wineman and Rajagopal, 2000). Using the strength of material approach an analytical solution is developed for a sandwich beam in three-point bending. This solution is extended to make it suitable for analyzing creep in a sandwich beam. The Correspondence Principle is used and leads to the formulation of the convolution integral. The convolution integral in the uniaxial state, sometimes referred to as the Boltzmann superposition principle, is generalized to multiaxial relations for isotropic materials.

Chapter III presents the FE solution to deformation in a linear viscoelastic sandwich beam. An analysis is performed using 2D continuum elements. The stipulation of plane strain is imposed for the 2D elements to solve for the time-dependent deformation in the sandwich beam. The model is tested numerically under three-point bending and the responses are compared to the ones obtained using analytical solution (Chapter II). A convergence study is also performed to determine accurate FE solutions.

The response between a sandwich system with aluminum skins and the one with FRP skins is studied.

Chapter IV presents analyses of the sandwich beam through parametric studies performed on the core and skin thickness, the ratio of skin to core moduli, the viscosity of the core foam and skins, and the sandwich beam with the addition of adhesive layers. The analyses determine the effect of the modified parameters on the overall performance and behavior of the sandwich beam.

Conclusions are reserved for chapter V.

CHAPTER II

ANALYTICAL SOLUTION TO THE PROBLEM OF DEFORMATION IN VISCOELASTIC SANDWICH BEAMS

This chapter presents the analytical solution for deformation in sandwich beams containing viscoelastic foam cores. The sandwich beams are comprised of linear elastic FRP skins and a viscoelastic polymer foam core. Governing equations of the deformation of viscoelastic materials will be represented in differential form and hereditary integral form. A single integral constitutive equation is used to model linear viscoelastic materials. For this reason, the Boltzmann superposition principle will be discussed. The mechanical responses of viscoelastic materials such as stress relaxation function, creep compliance function, and characteristic creep and relaxation times will also be discussed.

The analytical solution for bending in a sandwich beam is derived based on the strength of material approach. The Correspondence principle provides the means to convert linear elastic solutions into solutions for linear viscoelastic problems. Solutions to the linear viscoelastic problems can be obtained from corresponding linear elastic solutions through the use of the Laplace transform. The application of the Correspondence principle to the derived analytical solution for bending of a sandwich beam with a viscoelastic core will be discussed.

2.1 MECHANICAL RESPONSES OF VISCOELASTIC MATERIALS

A viscoelastic material is one in which both elastic solid and viscous fluid characteristics are exuded in the behavior of the material. For a solid like material, the rate of deformation ceases in time and an equilibrium or steady-state condition is reached. For viscoelastic fluids, the deformation continues to increase with time and at later times the material deforms at a constant velocity (Agosti, 2006; Mase, 1970). Linear viscoelasticity has been successfully used in representing the time-dependent mechanical behavior of materials under low stress and small deformations. Viscoelastic materials in the linear range permit the construction of creep function from a relaxation function and vice versa. The behaviors of linear viscoelastic materials are often described by mechanical analog models consisting of linear elastic springs and linear viscous dashpots. These models are suited to describe the deformation of various viscoelastic materials under uniaxial extension or pure shear loading (Mase, 1970; and Flügge, 1975). The one-dimensional constitutive equation for the linear elastic spring component, having a spring constant E, is:

$$\sigma = E \cdot \varepsilon \tag{2.1}$$

where E, σ, and ε are the elastic modulus, stress, and strain, respectively. The constitutive equation for the linear viscous component is:

$$\sigma = \eta \cdot \dot{\varepsilon} \tag{2.2}$$

where η and $\dot{\varepsilon}$ are viscosity and strain rate, respectively. Linear viscoelastic constitutive equations are formed by superimposing components with the constitutive equations given by Eqs. (2.1) and (2.2) (Chen, 2000; Wineman and Rajagopal, 2000). Responses of viscoelastic materials are characterized by spring-dashpot models consisting of several arrangements of elastic springs or viscous dashpots (Tschoegl, 1989; Betten, 2005; Christensen, 1982; Nuñez et al., 2004). Two basic forms of mechanical analog models used in the study of linear viscoelastic behavior are the Kelvin-Voigt and Maxwell models. The Kelvin-Voigt model consists of a spring and dashpot in parallel and the Maxwell model is made up of a combination of a spring and dashpot in series as shown in Fig. 2.1. The governing differential equation for the Kelvin-Voigt model is of the form:

$$\sigma = E \cdot \varepsilon + \eta \cdot \dot{\varepsilon} \tag{2.3}$$

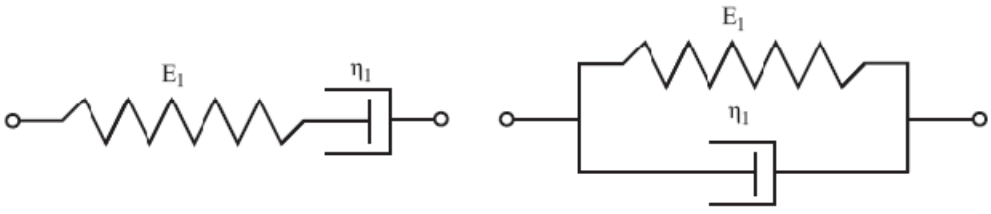

Fig. 2.1. Two basic forms of viscoelastic mechanical models; the Maxwell model, with a spring and dashpot in series and the Kelvin-Voigt model, with a spring and dashpot in parallel.

Equation (2.3) can be applied to either the shear or normal stress of the material. When a constant stress is applied to a viscoelastic material of the Kelvin-Voigt type, it deforms at a decreasing rate and the rate tends to zero as it approaches the steady state strain. Once the stress is removed, the material steadily returns back to its original state. The Kelvin-Voigt model cannot capture the instantaneous elastic response due to a constant stress. When the Kelvin-Voigt model is subjected to a sudden constant strain, it results in immediate relaxation to a constant stress (Shaw and MacKnight, 2005). The creep compliance and relaxation modulus of the Kelvin-Voigt model are of the form:

$$D(t) = \frac{1}{E}(1 - \exp^{-t/\tau_c}) \tag{2.4}$$

$$E(t) = \frac{\sigma(t)}{\varepsilon} = [\eta \cdot \delta(t) + E] \tag{2.5}$$

where τ_c, $D(t)$, $E(t)$, and are retardation time, creep compliance, and relaxation modulus, respectively. Where the retardation time τ_c is given as $\frac{\eta}{E}$ The Dirac delta function, $\delta(t)$ is applied and represents a generalized function having zero value everywhere except for at zero. Wineman and Rajagopal (2000) and Shaw and MacKnight (2005) stated that the instantaneous elongation of the model requires the viscous damper to instantly elongate and true relaxation is not possible, which would require an infinite force. For the stress relaxation, there is infinite stress applied over a short period in time and the Dirac delta function is used to represent with the instantaneous stress that immediately relaxes.

Therefore, this model cannot describe stress relaxation but it can be used to predict transient creep. The governing differential equation for the Maxwell model is of the form:

$$\dot{\varepsilon} = \frac{1}{E}\dot{\varepsilon} + \frac{\sigma}{\eta} \tag{2.6}$$

In this model, if the material is placed under a constant strain, the stress steadily relaxes to reach zero stress. Under a constant stress, there are two components for strain: (1) an elastic component that occurs instantaneously and (2) a viscous component that continuously increases with time as long as stress is applied. This behavior implies the model is for fluid like response. The creep compliance and stress relaxation for the Maxwell model are of the form:

$$D(t) = \frac{1}{E} + \frac{t}{\eta} \tag{2.7}$$

$$E(t) = E \cdot \exp^{-t/\tau_R} \tag{2.8}$$

where τ_R is a characteristic time referred to as the relaxation time and is equal to $\frac{\eta}{E}$.

Wineman and Rajagopal (2000) stated that the larger the value for τ_R, the slower the stress relaxes; therefore the relaxation time is a measure of how fast the stress relaxes. The Maxwell model can predict stress relaxation, but it cannot model creep behavior for

solids. The differential equations mentioned above are some forms of the general constitutive equations for linear viscoelastic behavior.

Simple Kelvin-Voigt and Maxwell models provide an inadequate representation of the behavior of viscoelastic solids because they do not have the ability to incorporate instantaneous elastic strain, show deformation with decreasing strain rates, relax steadily with time, or reach an equilibrium state in the case of relaxation. Therefore, it is necessary to choose other models for predicting the viscoelastic behavior of solids. A sufficient model of solid-like linear viscoelastic behavior requires a minimum of three elements, i.e., two springs and one dashpot while liquid-like behavior must be modeled with no less than four elements, i.e., two springs and two dashpots (Tschoegl, 1989). Several mechanical analog models encompassing the springs and dashpots have been developed to describe viscoelastic behavior. A standard three-parameter linear viscoelastic model, known as the SLS or Zener model can be represented in two ways; (a) a spring in series with a Kelvin unit or (b) a spring in parallel with a Maxwell unit. The SLS is the simplest model used to predict the viscoelastic behavior of a solid-like material and it has the ability to predict both creep and relaxation as shown in Fig. 2.2.

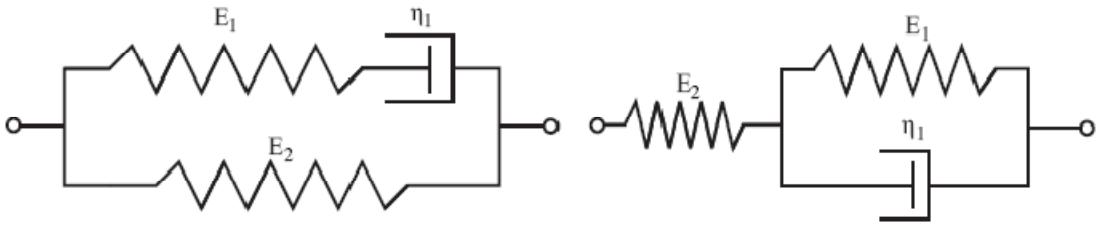

Fig. 2.2. SLS model with Maxwell and spring in parallel and with Kelvin and spring in series.

The governing differential equation for SLS model where a spring and Kelvin model are in series is:

$$\sigma\left(E_1 + E_2\right) + \eta\dot{\sigma} = E_1 E_2 \varepsilon + \eta E_2 \dot{\varepsilon} \tag{2.9}$$

where E_1 and E_2 are the instantaneous and equilibrium moduli, respectively. The creep compliance for the SLS model where a spring and Kelvin model are in series is:

$$D(t) = D_U + D_R(1 - \exp^{-t/\tau_C})$$
$$\text{where,} \quad D_U = \frac{1}{E_1}, \quad D_R = \frac{1}{E_2}, \quad \tau_C = \frac{\eta}{E_1} \tag{2.10}$$

The relaxation modulus is of the form:

$$E(t) = E_U + E_R \cdot \exp^{-t/\tau_R}$$
$$\text{where,} \quad E_R = \frac{E_1 E_2}{E_1 + E_2}, \quad E_U = E_2 \tag{2.11}$$

The strain reaches an equilibrium value under a constant stress and stress reaches equilibrium under a constant strain. So, it is implied that the SLS models represent the viscoelastic behavior of materials which reach an equilibrium value after ample time has elapsed following an imposed excitation.

Various forms of the four-parameter model exist. The Burgers model mentioned in Chapter I is extensively used in describing viscoelastic materials and consists of a Maxwell model and Kelvin-Voigt model in series as shown in Fig. 2.3. The Burgers model incorporates the instantaneous elastic response and the delayed elastic response, and it allows for the inclusion of permanent deformation upon removal of the loading.

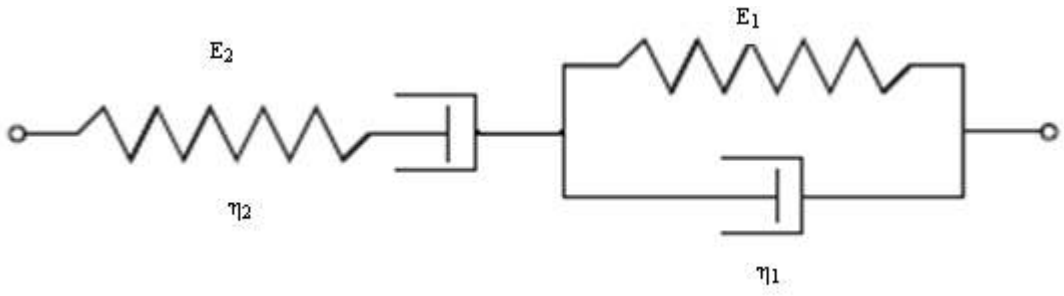

Fig. 2.3. A Maxwell model and Kelvin-Voigt in series form the four-parameter Burgers model (Hagin, 2003).

The relaxation modulus for the Burgers model is of the form:

$$E(t) = \frac{p_2}{A}\left(q - q_2\frac{p_1 - A}{2p_2}\right)\cdot \exp^{-\frac{p_1 - A}{2p_2}\cdot t} - \left(q_1 - q_2\frac{p_1 + A}{2p_2}\right)\cdot \exp^{-\frac{p_1 + A}{2p_2}\cdot t}$$

$$\text{where,}\quad A = \sqrt{p_1^2 - 4p_2},\ p_1 = \frac{\eta_1}{E_1} + \frac{\eta_1}{E_2} + \frac{\eta_2}{E_1},\ p_2 = \frac{\eta_1}{E_1}\frac{\eta_2}{E_2},\quad q_1 = \eta_1,\ q_2 = \frac{\eta_1\eta_2}{E_2} \tag{2.12}$$

The relaxation function is complex in comparison to the creep compliance, which is of the form:

$$D(t) = \frac{1}{E_1} + \frac{1}{E_2}(1 - \exp^{-t/\tau_C}) + \frac{t}{\eta} \tag{2.13}$$

Generalized versions of the Maxwell and Kelvin-Voigt models consisting of *n*-elements are used to improve the depiction of viscoelastic behavior by increasing the number of elements. The time-dependent functions for a generalized Maxwell or Kelvin-Voigt models are expressed in an exponential series, i.e., $\sum_{i=1}^{n} \beta_i \cdot \exp[-t/\tau_{C_i}]$, for a relaxation function. The exponential series representation is known as the Prony series. The Prony parameters are characterized by fitting experimental data.

To characterize mechanical properties of viscoelastic materials, creep, stress relaxation, and dynamic mechanical loadings are often performed (Agosti, 2006). A creep test consists of instantaneous application of a constant stress and the material strain

(deformation) is measured as a function of time. In a relaxation test an instantaneous constant strain is applied and the material stress (load) is measured as a function of time (Mase, 1970; Ferry, 1980; Shaw and MacKnight, 2005; Flügge, 1975; Wineman and Rajagopal, 2000). The characteristic creep and relaxation time is the time at which considerable stress relaxation or creep has occurred due to the unit step input loading (Wineman and Rajagopal, 2000).

A characteristic time can be examined and defined in various manners. Relaxation and retardation times are represented by τ, in which a subscript is usually given to distinguish between the two. Each characteristic time is related to a spectral strength such as the modulus E_i or the compliance $D_{i,}$ and the time-dependence of a material is revealed in a finite, discrete set of characteristic times and their related modulus or compliance (Tschoegl, 1997).

2.2 CONSTITUTIVE INTEGRAL MODEL FOR LINEAR VISCOELASTIC MATERIAL

In linear viscoelastic theory, the time-dependent response of a viscoelastic material can be expressed in an integral or a differential form. Linear viscoelastic functions can be represented by a Volterra hereditary integral that relates time-dependent stress and strain. Either the creep or the relaxation integral can be used to denote the linear viscoelastic characteristics of a material and therefore a relationship must exist between the two functions, i.e. creep and relaxation (Mase, 1970). In order to determine the stress or strain state in a viscoelastic material at any instant of time, the loading

histories need to be included. For a linear viscoelastic material, a superposition method is used to incorporate the history of the loading, which is described by a single integral representation known as the Boltzmann superposition principle (Ferry, 1980; Tschoegl, 1989). A response to an arbitrary input loading can be obtained by approximating the loading with multiple steps of input starting at different times. The creep strain response due to an arbitrary stress history is expressed by:

$$\varepsilon(t) = \sum_{i=1}^{N} \Delta\varepsilon_i(t) = \sum_{i=1}^{N} D(t-\tau_i)\Delta\sigma_i \tag{2.14}$$

and the summation leads to the integral form for a linear viscoelastic material under uniaxial loading when limit $\Delta\sigma_i \to 0$ and $N \to \infty$:

$$\varepsilon(t) = \int_0^t D(t-\tau)\frac{\mathrm{d}\sigma(\tau)}{\mathrm{d}\tau}\,\mathrm{d}\tau \tag{2.15}$$

Likewise, the relaxation stress response due to an arbitrary strain history is given as:

$$\sigma(t) = \sum_{i=1}^{N} \Delta\sigma_i(t) = \sum_{i=1}^{N} E(t-\tau_i)\Delta\varepsilon_i \tag{2.16}$$

The summation leads to the integral form for a linear viscoelastic material under uniaxial loading of the form:

$$\sigma(t) = \int_0^t E(t-\tau_i)\frac{\mathrm{d}\varepsilon(\tau)}{\mathrm{d}\tau}\,\mathrm{d}\tau \tag{2.17}$$

In the above equations, $D(t)$ and $E(t)$ are one dimensional (1D) creep compliance and stress relaxation, respectively. Equations (2.16) and (2.18) are valid when stress and strain histories are smooth functions of time. When there is discontinuity (jump) in the input loading, say at $t = 0$, the expressions for the time-dependent strain and stress are given as:

$$\varepsilon(t) = D(0)\sigma(t) + \int_0^t D(t-\tau)\frac{\mathrm{d}\sigma(\tau)}{\mathrm{d}\tau}\,\mathrm{d}\tau \tag{2.18}$$

$$\sigma(t) = E(0)\varepsilon(t) + \int_0^t E(t-\tau_i)\frac{\mathrm{d}\varepsilon(\tau)}{\mathrm{d}\tau}\,\mathrm{d}\tau \tag{2.19}$$

The relationship between the creep and relaxation functions can be determined by using the Laplace transform. The compliance and modulus material parameters are reciprocals of each other, but this is not the case for the time-dependent functions. Mathematically, the relationship between $E(t)$ and $D(t)$ can be obtained by noting that due to a unit of $\sigma(t) = 1$, the strain is $\varepsilon(t) = 1 \cdot D(t)$. When $t \geq 0$ the integral is of the form:

$$1 = D(0)E(t) + \int_0^t E(t-\tau)\frac{\mathrm{d}D(\tau)}{\mathrm{d}\tau}\,\mathrm{d}\tau \tag{2.20}$$

Likewise, an equivalent relation is obtained by applying a unit of strain $\varepsilon(t) = 1$, the stress output is $\sigma(t) = 1 \cdot E(t)$. The integral model in Eq. (2.20) reduces to:

$$1 = E(0)D(t) + \int_0^t D(t-\tau)\frac{\mathrm{d}E(\tau)}{\mathrm{d}\tau}\,\mathrm{d}\tau \tag{2.21}$$

The above equations are the integral relations between the stress relaxation and creep compliance functions. The Laplace transform is applied to the above hereditary integrals, where for creep, the strain is of the form:

$$\varepsilon(s) = L\left\{\int_0^t D(t-\tau)\frac{\mathrm{d}\sigma(\tau)}{\mathrm{d}\tau}\,\mathrm{d}\tau\right\} = D(s)\cdot s\sigma(s) \tag{2.22}$$

and relaxation for stress is of the form:

$$\sigma(s) = L\left\{\int_0^t E(t-\tau)\frac{\mathrm{d}\varepsilon(\tau)}{\mathrm{d}t}\,\mathrm{d}t\right\} = E(s)\cdot s\varepsilon(s) \tag{2.23}$$

where,

$$\sigma(s) = E(s) \cdot s\varepsilon(s) = E(s) \cdot sD(s)s\sigma(s) \tag{2.24}$$

The linear viscoelastic relationship between stress relaxation and creep compliance is then found to be:

$$D(s)E(s) = \cdot \frac{1}{s^2} \tag{2.25}$$

Equation (2.26) is the Laplace transform of:

$$\int_0^t D(t-\tau)E(\tau)\mathrm{d}\tau = \int_0^t E(t-\tau)D(\tau)\mathrm{d}\tau = t \tag{2.26}$$

It is noted that the stress relaxation $E(t)$ decreases monotonically and the creep compliance $D(t)$ increases monotonically. The relationship between the creep compliance and stress relaxation is:

$$D(t)E(t) \leq 1 \tag{2.27}$$

where reciprocity only holds true for $t = 0$ and $t \rightarrow \infty$ (Partl, 2006; Wineman and Rajagopal, 2000). The creep compliance and stress relaxation are not reciprocal for intermediate moments of time (Partl, 2006).

The superposition principle is limited to linear materials in which the following conditions are satisfied: (1) the material experiences small deformation gradients, (2) the material properties are independent of mechanical loadings i.e. stress is proportional to strain, (3) the material properties are independent of the time when loading starts i.e. non-aging materials, and (4) the temperature is constant (Partl, 2006). Even though Boltzmann's superposition principle is limited to linear viscoelastic responses, it can be extended for use in nonlinear behavior as well. The superposition principle is modified for use in nonlinear solutions for viscoelastic materials, e.g., Schapery integral model.

As discussed by Wineman and Rajagopal (2000), the effect of the property of linearity was that responses to separate histories of stress and strain components could be superposed and the same holds true for linearity in the 3D behavior of materials. A single integral constitutive relation is used in this study to model uniaxial viscoelastic behavior. The uniaxial viscoelastic relation is generalized for the multiaxial 3D constitutive relations by separating the deviatoric and volumetric strain-stress relations (Joshi, 2008; Haj-Ali and Muliana, 2004). These relations are expressed as:

$$
\begin{aligned}
\varepsilon_{ij}^{t} &= e_{ij}^{t} + \frac{1}{3} e_{kk}^{t} \delta_{ij}^{t} \\
e_{ij}^{t} &= \frac{1}{2}(\sigma^{t}) J_0 S_{ij}^{t} + \frac{1}{2}(\sigma^{t}) \int_0^t \Delta J(t-\tau) \frac{\mathrm{d}S_{ij}^{t}}{\mathrm{d}\tau}\,\mathrm{d}\tau \\
e_{ij}^{t} &= \frac{1}{3}(\sigma^{t}) B_0 \sigma_{kk}^{t} + \frac{1}{3}(\sigma^{t}) \int_0^t \Delta B(t-\tau) \frac{\mathrm{d}\sigma_{kk}^{t}}{\mathrm{d}\tau}\,\mathrm{d}\tau
\end{aligned}
\tag{2.28}
$$

The parameters e_{ij}, ε_{kk}, S_{ij}, and σ_{kk} represent the deviatoric strains, volumetric strains, deviatoric stresses, and volumetric stresses, respectively. The instantaneous elastic shear and bulk material parameter are represented by J_0 and B_0, respectively. It is assumed that the corresponding linear elastic Poisson's ratio is time-independent. Thus, the time-dependent shear and bulk compliances are represented by ΔJ and ΔB, respectively, and are of the form:

$$\Delta B^t = 2(1+\nu)\Delta D^t \qquad B_n = 2(1+\nu)D_n \tag{2.29}$$

$$\Delta J^t = 2(1+\nu)\Delta D^t \qquad J_n = 2(1+\nu)D_n \tag{2.30}$$

The uniaxial time-dependent compliance is represented by various functions, a few of which are the power law, exponential, and Prony series. The Prony series representation for a creep function is:

$$\Delta D^t = \sum_{n=1}^{N} D_n (1 - \exp[-\lambda_n t]) \tag{2.31}$$

where N is the number of terms, D_n is the n^{th} coefficient of the Prony series, and λ_n is the n^{th} reciprocal of retardation time. By using Eqs. (2.30) and (2.31), the deviatoric and volumetric strains in Eq. (2.29) can be represented as:

$$e_{ij}^{t} = \frac{1}{2} J_0 S_{ij}^{t} + \frac{1}{2} S_{ij}^{t} \sum_{n=1}^{N} J_n - \frac{1}{2} \sum_{n=1}^{N} J_n q_{ij,n}^{t}$$

$$\text{where,} \quad q_{ij,n}^{t} = \int_0^t \exp[-\lambda_n (t-\tau)] \frac{\mathrm{d}S_{ij}^{t}}{\mathrm{d}\tau} \mathrm{d}\tau \tag{2.32}$$

$$\varepsilon_{kk}^{t} = \frac{1}{3} B_0 \sigma_{ij}^{t} + \frac{1}{3} \sigma_{kk}^{t} \sum_{n=1}^{N} B_n - \frac{1}{3} \sum_{n=1}^{N} B_n q_{kk,n}^{t}$$

$$\text{where,} \quad q_{ij,n}^{t} = \int_0^t \exp[-\lambda_n (t-\tau)] \frac{\mathrm{d}S_{ij}^{t}}{\mathrm{d}\tau} \mathrm{d}\tau \tag{2.33}$$

The numerical solutions to Eqs. (2.33) and (2.34) are obtained by using a recursive method shown by Haj-Ali and Muliana (2004). These solutions are implemented in a general FE analysis.

2.3 ANALYSIS OF THE DEFORMATION IN VISCOELASTIC SANDWICH BEAMS UNDER BENDING

The analytical solution to the deformation in a viscoelastic sandwich beam subjected to three-point bending can be obtained from the strength of material approach with the use of the Correspondence Principle (Rocca and Nanni, 2004). A sandwich beam is comprised of two skins and a core, where *t*, *c*, *h*, *b,* and *d* are the thickness of each skin, thickness of the core, the depth, the width, the distance between the centerlines of both skins and the length, respectively is shown in Fig. 2.4. The strength of material approach will first be used to introduce equations that represent a sandwich beam having linear elastic skins and a linear elastic core. It is assumed that cross

sections remain plane and perpendicular to the longitudinal axis before and after bending.

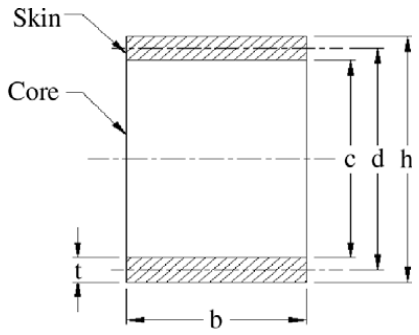

Fig. 2.4. Sandwich beam geometry (Raju et al., 2006).

Bending and shear components make up the total transverse deformation of the beam. The flexural rigidity of the beam, *EI* or *D*, is determined. For a sandwich beam *D* is the sum of the flexural rigidities of the skins and core measured about the centroidal axis of the entire beam:

$$D = \underbrace{\frac{E_f bt^3}{6} + \frac{E_f btd^2}{2}}_{\text{stiffness of the faces}} + \underbrace{\frac{E_c bc^3}{12}}_{\text{stiffness of the core}} \tag{2.34}$$

where E_f and E_c are the Young's moduli of the skin and core, respectively. If it is assumed that the sandwich beam is relatively thin, in which the first and last terms of Eq.

(2.35) amount to less than 1 percent of the second term, then the first and third terms and may be ignored if both the conditions in Eqs. (2.36) and (2.37) are fulfilled.

$$3 \cdot \left(\frac{d}{t} \right)^2 > 100 \tag{2.35}$$

$$\frac{E_f}{E_c} \cdot \frac{td^3}{c^3} > 16 \tag{2.36}$$

If both the conditions in Eqs. (2.36) and (2.37) are fulfilled, the flexural rigidity reduces to:

$$(EI)_{eq} = D = E_f \cdot \frac{btd^2}{2} \tag{2.37}$$

Figure 2.5 shows a simply supported sandwich beam subjected to a midspan load, *P* which represents three-point bending. To determine the deformation at the midspan of the structure (*L/2*), the bending component and the shear deformation are accounted for and the elastic deformation is derived from:

$$\delta = \underbrace{\frac{PL^3}{48D}}_{\text{bending component}} + 1.2 \underbrace{\frac{PL}{4(AG_c)}}_{\text{shear component}} \quad \text{where, } A = bd \tag{2.38}$$

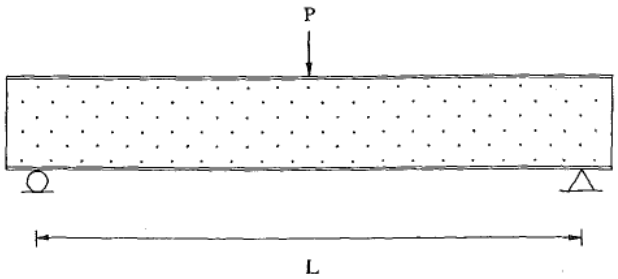

Fig. 2.5. Simply supported sandwich beam with a concentrated point load at the midspan for three-point bending (Huang and Gibson, 1990).

where D, P, L, and A, and G_C are the equivalent flexural rigidity, load, length of beam, cross-sectional area, and shear modulus of the core, respectively. The shear correction factor, k, is represented by 1.2 for a rectangular cross-section. The same equations used to determine the deformation in the sandwich beam with linear elastic skins and core are also used in determining the deformation in a sandwich beam with linear elastic skins and a linear viscoelastic foam core. Huang and Gibson (1990) show that the bending component of the deformation remains the same while the shearing component increases with time as the shear modulus of the viscoelastic core is efficiently reduced. The equation for the creep bending deformation of the sandwich beam subjected to three-point bending is given by:

$$\delta = \frac{PL^3}{48D} + 1.2\frac{PLJ_c(t)}{4A} \tag{2.39}$$

where $J_C(t)$ is the shear creep compliance of the core.

Using the strength of material approach, the time-dependent deformation for a sandwich beam with linear elastic skins and a viscoelastic core was determined. To accomplish this, a 1000 mm long and 200 mm wide sandwich beam composed of 0.5 mm thick aluminum skins and 50.8 mm thick polystyrene foam core is subjected to a three-point bending test with a point load of 1000 N applied at the midspan of the beam. The numerical creep compliance data for polystyrene reported by Plazek and O'Rourke was used to calibrate the time-dependent parameters using a Prony series (Ferry, 1980). The time-dependent material properties for the polystyrene foam are given in Table 2.1. Elastic properties for the polystyrene foam core and aluminum skins are given in Table 2.2. The response from the analytical solution corresponds with the experimental data as shown in Fig. 2.6

Table 2.1
Calibrated Prony series coefficients for the polystyrene foam core (shear creep compliance)

n	λ_n (hr^{-1})	$J_n \times 10^{-2}$ (MPa^{-1})
1	1	5.00
2	10^{-1}	99.9
3	10^{-2}	175
4	10^{-3}	133
5	10^{-4}	100
6	10^{-5}	100
7	10^{-6}	200
8	10^{-8}	3500

The equilibrium compliance: $J_0 = 1.35 \times 10^{-3}$ (MPa^{-1})

Table 2.2
Polystyrene and aluminum elastic material properties

	E, Young's Modulus (MPa)	*v*
Aluminum	70,000	0.35
Polystyrene	2,000	0.33

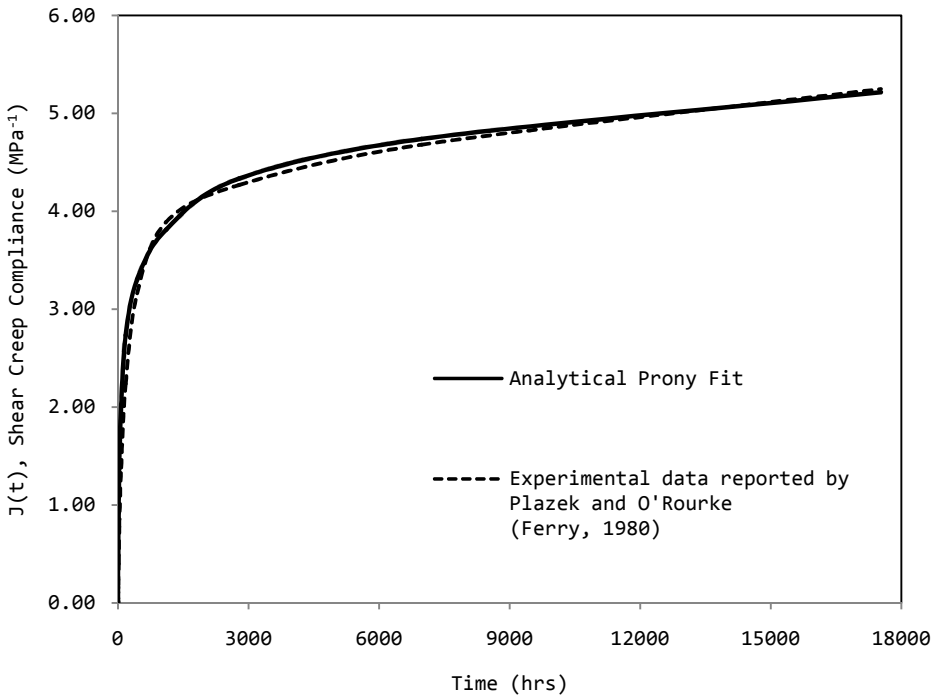

Fig. 2.6. Comparison of experimental and analytical data for the shear creep compliance of the polystyrene foam core.

2.4 CORRESPONDENCE PRINCIPLE

Analytical calculations were based on the strength of material approach for linear elastic materials, and the Correspondence Principle was used to obtain a solution for linear viscoelastic materials. The Correspondence Principle provides the means to convert the elastic linear solutions into solutions for linear viscoelastic problems, but there are conditions that must exist in order for the Correspondence Principle to be applicable. In order to apply the Laplace transform; the displacement must be defined at all times for $t \geq 0$, the motion of the viscoelastic body must remain in equilibrium, and at a fixed point on the boundary the conditions should not change over time. Solutions to linear viscoelastic problems can be obtained directly from the corresponding linear elastic solutions through the use of the Laplace transform. Material parameters in the linear elastic solutions are replaced by a product of Laplace transformed variables of solutions to viscoelastic problems. The solutions are transformed back to the time domain solutions.

For bending deformation in a sandwich beam, if the deformation of the elastic beam is known, then the viscoelastic beam deformation can be found using the Correspondence Principle (Wineman and Rajagopal, 2000). Equation (2.39) represents the elastic deformation of a sandwich beam and it can be converted to the Laplace transform of the solution of the problem for viscoelastic deformation by making basic substitutions. As for the material properties, Poisson's ratio will be held constant but the shear modulus will be converted to a time-dependent material property. The field variable representing the deformation will also become time-dependent. In the shear

component of Eq. (2.39), G_C is converted to the Laplace transform by making the following replacement:

$$G_C \rightarrow s\overline{G}_C(s) \tag{2.40}$$

The field variables representing deformation are converted to the Laplace transform by making the following replacements:

$$\delta \rightarrow \overline{\delta}(s) \tag{2.41}$$

$$P \rightarrow \overline{P}(s) \tag{2.42}$$

After converting the shear modulus and field variables to the Laplace transform Eq. (2.39) becomes:

$$\overline{\delta}(s) = \frac{\overline{P}(s)L^3}{48D} + 1.2\frac{\overline{P}(s)L}{4As\overline{G}(s)} \qquad \text{where, } s\overline{G}(s) = \frac{1}{s\overline{J}(s)} \tag{2.43}$$

Since creep compliance is of interest, Eq. (2.44) is rewritten in the form:

$$\overline{\delta}(s) = \frac{\overline{P}(s)L^3}{48D} + 1.2\frac{\overline{P}(s)Ls\overline{J}(s)}{4A} \tag{2.44}$$

So, Eq. (2.45) can be inverted to give the deformation for the viscoelastic sandwich beam:

$$\delta(t) = \frac{P(t)L^3}{48D} + 1.2\frac{L}{4A}\int_0^t J_C(t-\tau)\frac{\mathrm{d}P}{\mathrm{d}\tau}\,\mathrm{d}\tau \tag{2.45}$$

CHAPTER III

NUMERICAL SOLUTION TO THE PROBLEM OF DEFORMATION IN LINEAR VISCOELASTIC SANDWICH BEAMS

This chapter presents the FE solution to deformation in a sandwich beam having linear elastic skins and a linear viscoelastic polymer core. The FE analysis is performed using 2D continuum plane strain elements. The time dependent deformation in the sandwich beam due to a concentrated force is monitored. The FE model is tested numerically under three-point bending and the responses, i.e, stresses, strains, and deformations, are compared to the those obtained using the analytical solution from Chapter II. Convergence studies are first performed to determine the accuracy of the FE solutions. Two sandwich systems are studied. The first sandwich beam consists of aluminum skins and polystyrene core material. Both aluminum and polystyrene are modeled as isotropic materials. The second sandwich beam is comprised of Graphite epoxy (GR/E) laminate skins and polystyrene core. The GR/E laminate skins are treated as orthotropic linear elastic skins. Thicknesses of the skins and core in both sandwich systems are the same. The GR/E laminate has higher elastic modulus in the longitudinal direction compared to aluminum. Elastic moduli of both skin materials are much higher than the modulus of the core.

3.1 FINITE ELEMENT MODEL FOR 2D VISCOELASTIC SANDWICH BEAM

The FE analysis was performed using ABAQUS, a commercial FE code. In this study, the mechanical constitutive behavior of the viscoelastic materials is defined using a user subroutine, i.e., UMAT. The UMAT is a numerical algorithm derived based on implicit stress integration solutions within general displacement based FE analyses (Joshi, 2008). During the time-dependent simulation, the UMAT must update the stresses, consistent tangent stiffness matrix, and history variables. In Joshi (2008), the FE analysis was used to solve the coupled problem of moisture diffusion and deformation in a sandwich beam. This study used 2D (CPE4) and three-dimensional (3D) (C3D8) elements. In Fig. 3.1, the 3D results for the transverse displacement are in agreement with the 2D results. Since the 2D and 3D results are in agreement, computational time is reduced by performing the analysis with 2D elements.

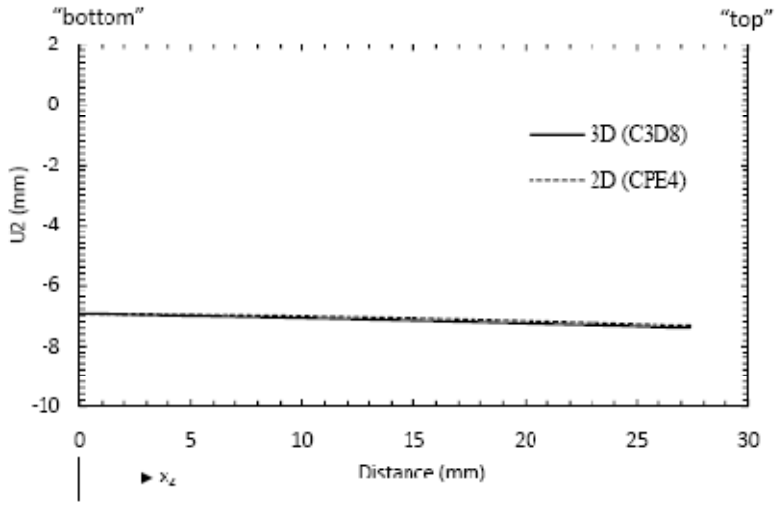

Fig. 3.1. Comparison of transverse displacement for 2D and 3D elements at 1200 hours (Joshi, 2008).

The input to the UMAT subroutine is the extensional compliance material property, $D(t)$. Experimental data for the polystyrene foam (Chapter II) was given in terms of the shear compliance material property. After fitting the experimental data with a Prony series, the extensional compliance was determined from the shear compliance by assuming the corresponding linear elastic Poisson's ratio constant. The shear compliance was converted to the extensional compliance. The calibrated Prony series is shown in Table 3.1. Elastic material properties for the aluminum skins and the polystyrene core are shown in Table 2.2. The sandwich beam in the study was modeled in ABAQUS using 2D plane strain elements (CPE4). In a plane strain condition, it is assumed that the out-of-plane strain component is zero. The plane strain element is suitable to generate a 2D model of a structure whose out-of-plane thickness is much larger than the other in-plane dimensions. Figure 3.2 shows the prescribed loading and boundary conditions used to simulate the sandwich beam under three-point bending.

Table 3.1
Calibrated Prony series coefficients for the polystyrene foam core (extensional compliance)

n	λ_n (hr^{-1})	$D_n \times 10^{-2}$, MPa^{-1}
1	1	1.88
2	10^{-1}	37.5
3	10^{-2}	65.8
4	10^{-3}	50.0
5	10^{-4}	37.6
6	10^{-5}	37.6
7	10^{-6}	75.2
8	10^{-7}	1320

The equilibrium compliance: $D_0 = 5.00 \times 10^{-4}$ MPa^{-1}

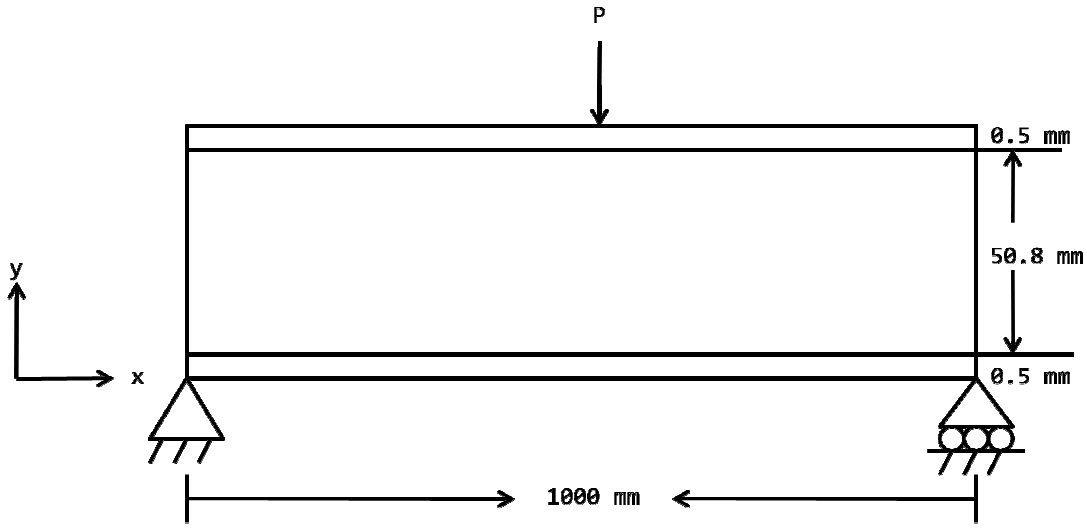

Fig. 3.2. Loading and boundary conditions for the sandwich beam.

3.2 CONVERGENCE STUDY USING FINITE ELEMENT ANALYSIS

It is essential to check the sufficiency of the number of elements, size of the elements, and time increment used in the FE model. The FE analysis is used to obtain variables, such as deformation, stress, and strain when the sandwich beam is subjected to three-point bending. A 1000 mm long and 200 mm wide sandwich beam composed of 0.5 mm thick aluminum skins and 50.8 mm thick viscoelastic polystyrene core is subjected to a three-point bending test. The beam is simply supported and has a point load of 1000 N applied at the midspan. Table 2.1 gives the calibrated Prony series for the analytical data and as mentioned in Section 3.1, the compliance is calibrated from the experimental data as the shear compliance material property, $J(t)$. The UMAT implemented in the FE code requires the compliance to be inputted as $D(t)$. The time-

dependent calibrated Prony series used for the FE analysis for the core is shown in Table 3.1. Elastic properties for the aluminum and polystyrene are shown in Table 2.2.

The appropriate initial time increment had to be chosen for the model. This value was adjusted until the instantaneous deformation for the FE model was close to the analytical instantaneous deformation. An initial (static) time increment of 1e-5 hours was used for this study. Table 3.2 shows the initial (static) time increments used in determining the appropriate instantaneous deformation. Once the appropriate instantaneous time increment was determined another convergence study was completed involving the refinement of the FE mesh. An increase in the density of the mesh, i.e., an increase in the number of elements, provides smoother variation of the field variables in the sandwich beam, which results in more accurate response prediction. The creep deformation for the analytical study and FE meshes consisting of 500 and 600 elements through the length is shown in Fig. 3.3. Creep deformation of sandwich beam with 600 elements through the length is about 1% higher than the creep deformation of sandwich beam with 500 elements through the length. Since the creep deformation increased insignificantly with the addition of 100 elements through the length, the time-dependent deformation in the FE study converged. The Mesh 1 (500) and Mesh 2 (600) FE models contain a total of 8000 and 19200 elements, respectively. With a constant load applied, the creep deformation continuously increases and therefore does not reach a point of steady-state. Eventually, the sandwich beam will reach a critical point at which failure starts.

Table 3.2
Comparison of instantaneous time and deformation for convergence study

Analytical Instantaneous Time (hrs)	Analytical Deformation (mm)
0	1.574
FE Instantaneous Time (hrs)	**FE Deformation (mm)**
1e-4	1.393
1e-5	1.593
1e-6	1.919

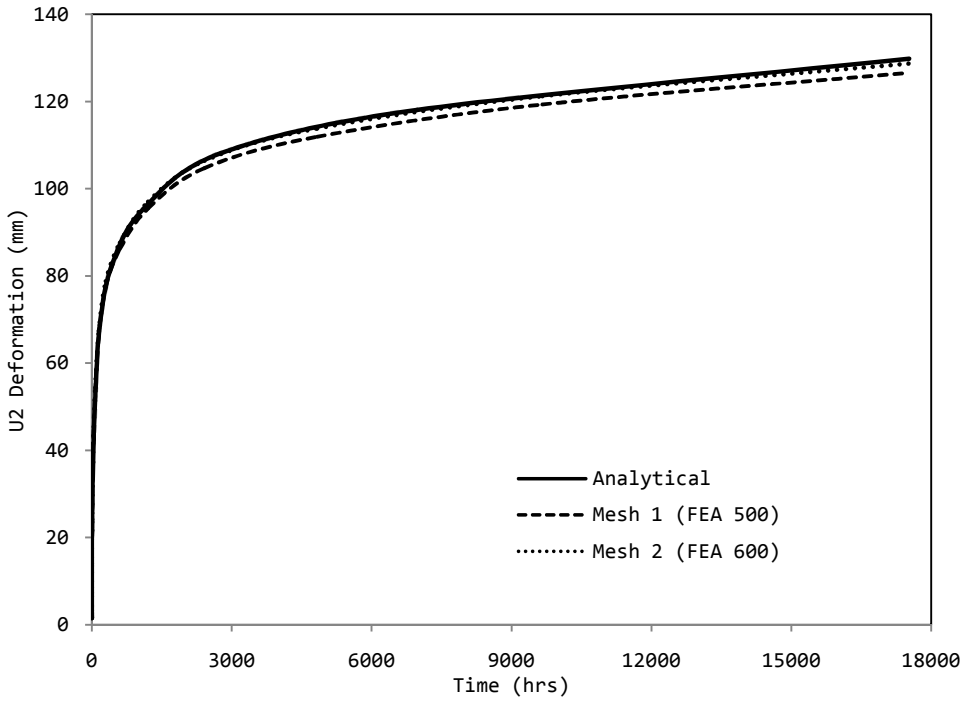

Fig. 3.3. Comparison of analytical and FE creep deformation for a sandwich beam with mesh refinement.

3.3 COMPARISON OF THE FINITE ELEMENT AND ANALYTICAL SOLUTIONS

The FE results in terms of stress, strain, and deformation are compared and verified with the analytical solution from Chapter II. The strength of material approach mentioned in Chapter II, is based on the Timoshenko beam theory (TBT) which takes into account the effect of shear deformation. The Euler-Bernoulli beam theory (EBT) is accurate for calculating the load-carrying and deformation characteristics of a beam and only accounts for flexural rigidity or bending effect which is applicable for slender beams. In Figure 3.4 (a), the analytical creep deformation was derived inclusive of the shear coefficient (k). Figure 3.4 (b) shows the analytical creep deformation exclusive of the shear coefficient. During the elastic instantaneous period the analytical and FE deformations of 1.574 mm and 1.593 mm, respectively, differ by 0.019 mm. The time-dependent deformation is mainly controlled by the shear deformation of the foam core.

The shear coefficient accounts for the non-uniform distribution of shear stress and strain through the cross-section of the sandwich beam (Schniepp, 2002). Numerical shear coefficients are calculated based on variations in the heigth to width ratio of the cross-section in a beam (Brancheriau, 2006). Brancheriau (2006) stated that Timoshenko defined k as the ratio of the average shear strain on a section to the shear strain at the centroid and concluded the k value to be 2/3 for a homogeneous beam with a rectangular cross-section. However, other approximations have been proposed for the k value and 5/6 is most commonly used as the value of k for beams with a rectangular cross-section.

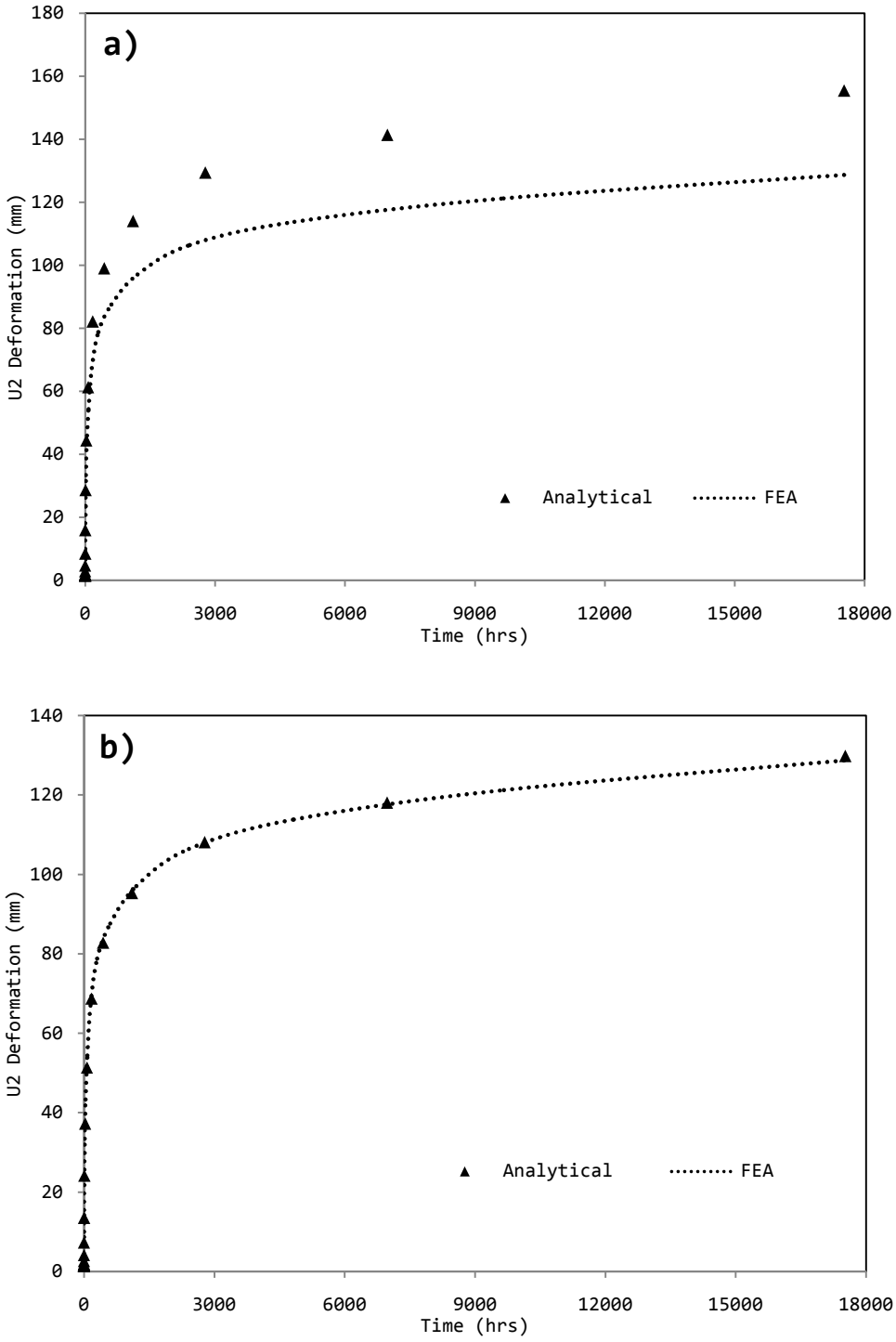

Fig. 3.4. Comparison of analytical and FE creep deformation for a sandwich beam (a) analytical analysis includes a shear correction factor (k) of 1.2 and (b) shear coefficient (k) is assumed to be 1.

The actual shear stress distribution is nonlinear through the thickness which depends on the geometrical properties of the beams, i.e., slender or stocky beam. When the shear constant $k = 5/6$ is used, it is assumed that the shear stress distribution is uniform through the thickness and the shear constant is used to adjust the proper value. Due to the inclusion of k in the analytical study, the analytical and FE solutions differed. An assumed value of one was used for the FE analysis. It is noted that the above k values were derived for homogeneous beams, while this study deals with heterogeneous beam. Thus, assuming a constant shear stress deformation may lead to significant error predictions.

3.4 DEFORMATION IN THE VISCOELASTIC SANDWICH BEAM WITH ALUMINUM SKINS VERSUS GRAPHITE EPOXY LAMINATE SKINS

Time-dependent studies were performed for the sandwich beam with aluminum skins and GR/E laminate skins. A sandwich beam of 1000 mm long and 200 mm wide is composed of 0.5 mm thick skins and 50.8 mm thick polystyrene core is subjected to a three-point bending test. The aluminum skins are linear elastic and the GR/E laminate skins are orthotropic elastic. In both sandwich beams linear viscoelastic polystyrene is used as the core material. Material properties for aluminum and polystyrene are shown in Table 2.2. The material properties for GR/E laminate are shown in Table 3.3. The beam is simply supported and has a point load of 1000 N applied at the midspan. Both sandwich beams are subject to the same loading and the boundary conditions are the same those shown in Figure 3.2.

In Figure 3.5, the transverse creep deformation is shown for the sandwich beams containing each skin material. Although the deformations are close, the sandwich beam with the laminate skins produced less creep deformation than the aluminum. The GR/E laminate skin has a higher elastic modulus in the axial fiber direction than the aluminum. When the longitudinal elastic modulus for GR/E laminate is compared to the elastic modulus for aluminum, it is almost 3 times larger. So, in the case of the three-point bending studies being analyzed the difference in strength would definitely make an impact on the deformation as well as the stresses and strains for the sandwich beam. The purpose of adding thin skins with higher stiffness is to carry the maximum normal stresses for beams under bending, while the thick core is intended to increase overall flexural rigidity of the beam. The Ultimate Tensile Strength (UTS) for aluminum is 276 MPa, while the UTS of GR/E laminate is equal to 1500 MPa in the longitudinal fiber direction. Failure occurs when the materials reaches stresses above the UTS. At stresses above the yield strength of the material, permanent deformation could occur even when the load is removed. For safety measures, constituents in a sandwich beam are designed with the yield strength in mind.

Table 3.3
Material properties of graphite epoxy laminate (T300/5208) (Yeh and Kim, 1994)

	GR/E
E_x (MPa)	1.81e5
E_y (MPa)	1.03e4
E_z (MPa)	1.03e4
v_x	0.30
v_y	0.28
v_z	0.28
G_x (MPa)	7.17e3
G_y (MPa)	4.00e3
G_z (MPa)	7.17e3

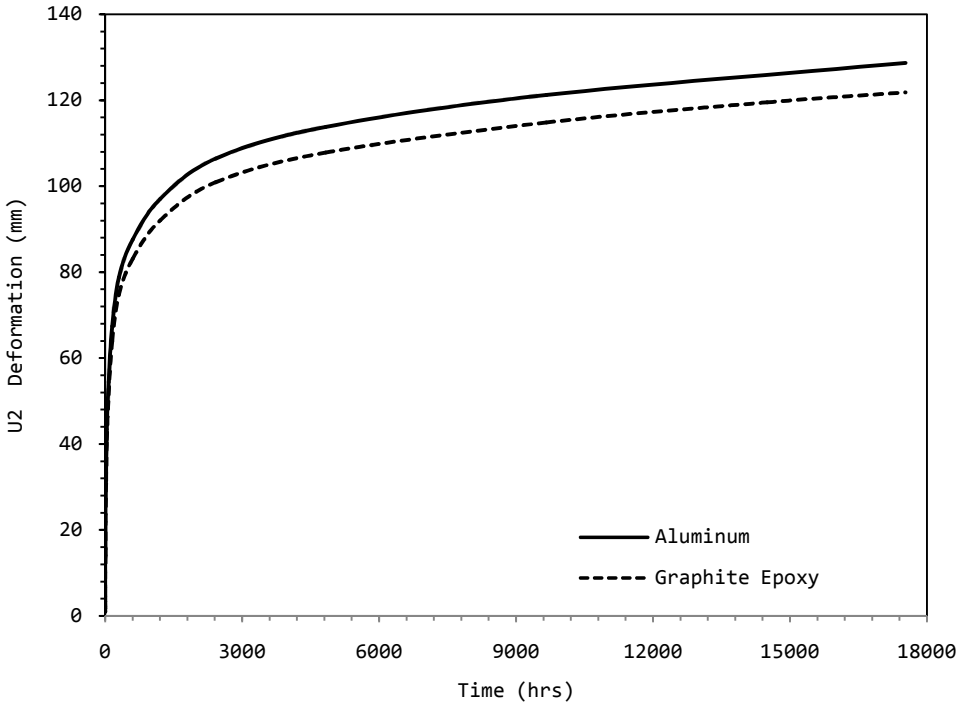

Fig. 3.5. Comparison of creep deformation for a sandwich beam with aluminum skins versus graphite epoxy laminate skins.

Localized stress concentration is observed near regions where the load and constraints are applied. Thus, the stresses and strains are measured at a distance of 83.3 mm away from the midspan of the sandwich beam where the effect of stress concentration is practically insignificant. If the responses are monitored near the placement of the point load, they are susceptible to stress concentrations. Even though the responses are monitored at a distance of 83.3 mm from the midspan, it is possible that they are still influenced by stress concentrations at the midpan created by the applied load. Figures 3.6 through 3.13 show how the field variables (stress, strain, and displacement) are varied in the sandwich beam. In Fig. 3.13, using a contour plot of the von Mises stress it can be seen that even though the field variables are monitored at distance of 83.3 mm from the midspan, it still may be close enough to experience the effect of stress concentration which explains the nonsymmetrical stress and strain plots with respect to the neutral axis.

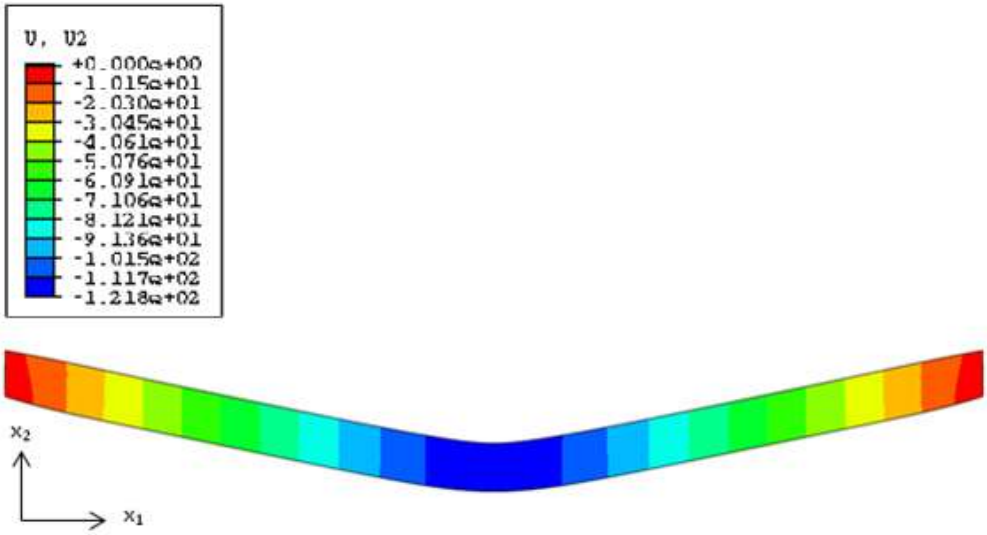

Fig. 3.6. Contour plot of transverse displacement (U_2) at 17530 hours (approximately 2 years).

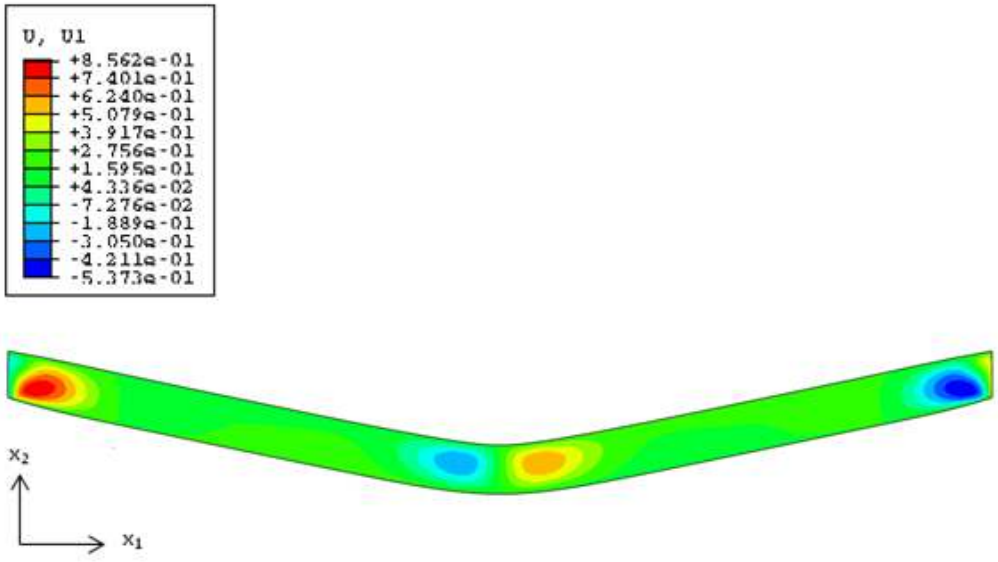

Fig. 3.7. Contour plot of longitudinal displacement (U_1) at 17530 hours (approximately 2 years).

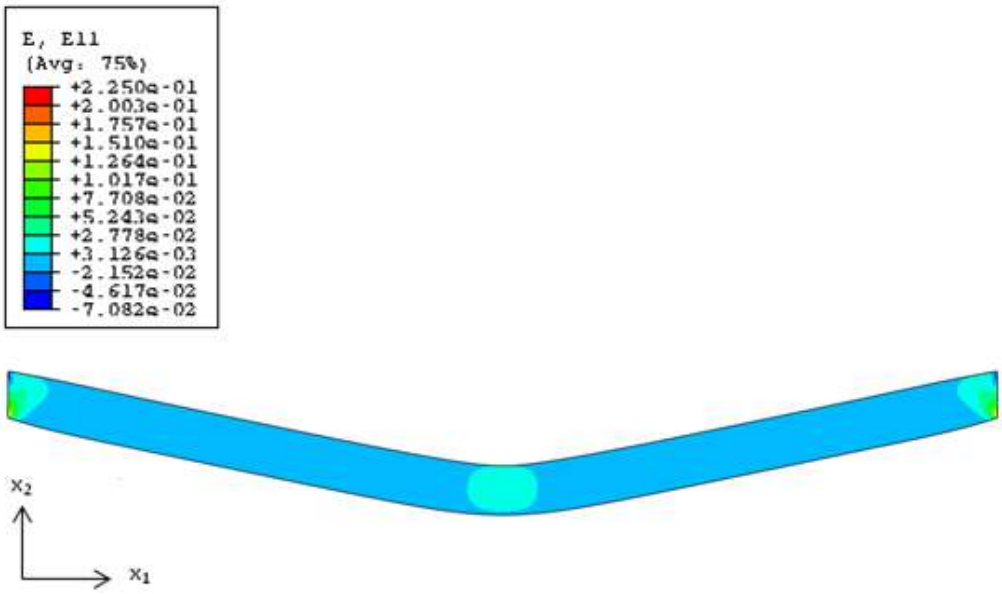

Fig. 3.8. Contour plot of longitudinal strain (E_{11}) at 17530 hours (approximately 2 years).

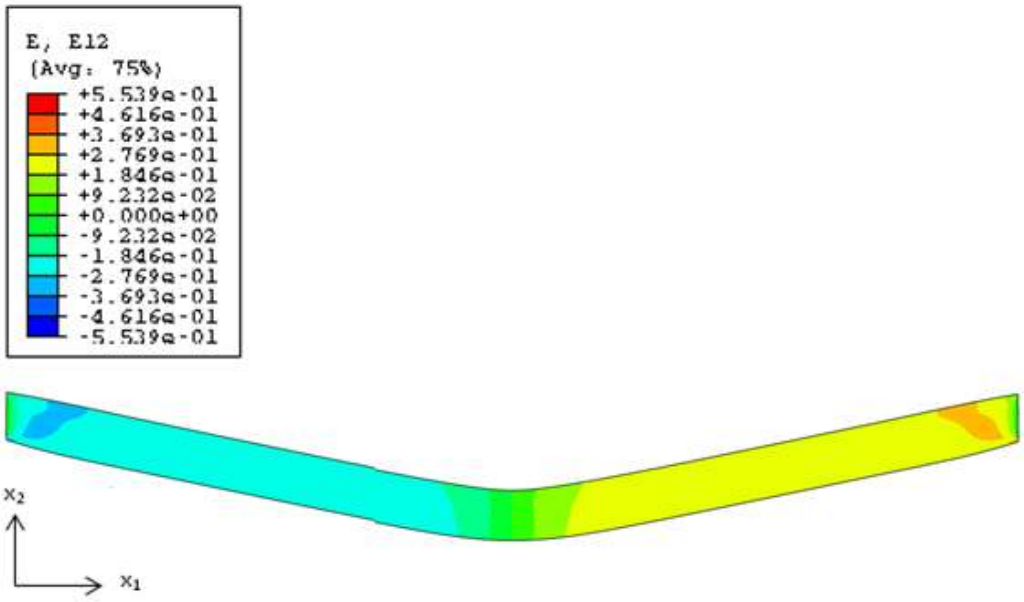

Fig. 3.9. Contour plot of shear strain (E_{12}) at 17530 hours (approximately 2 years).

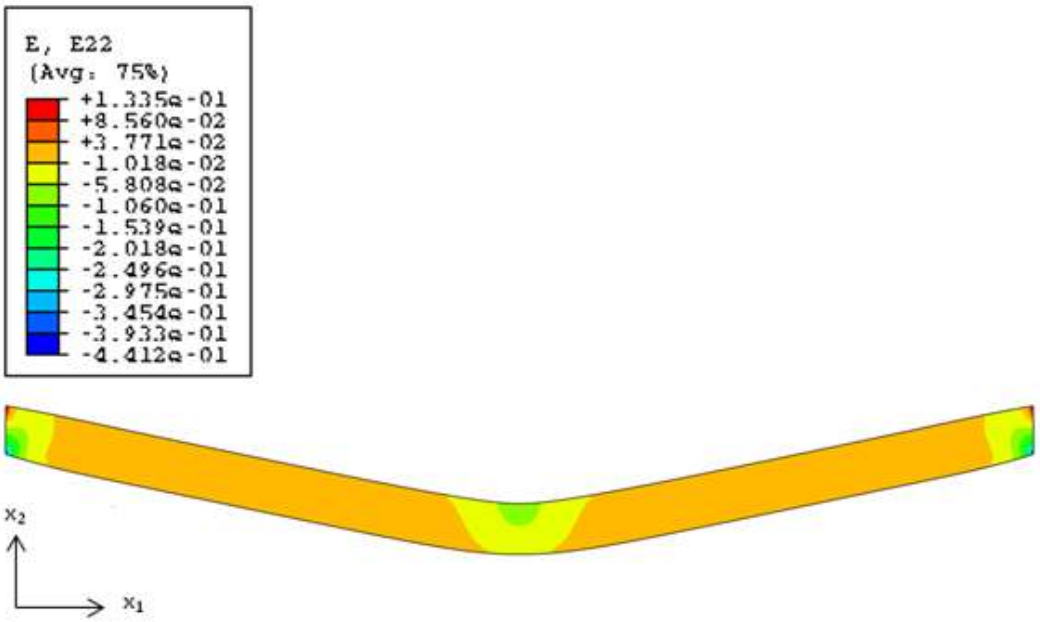

Fig. 3.10. Contour plot of transverse strain (E_{22}) at 17530 hours (approximately 2 years).

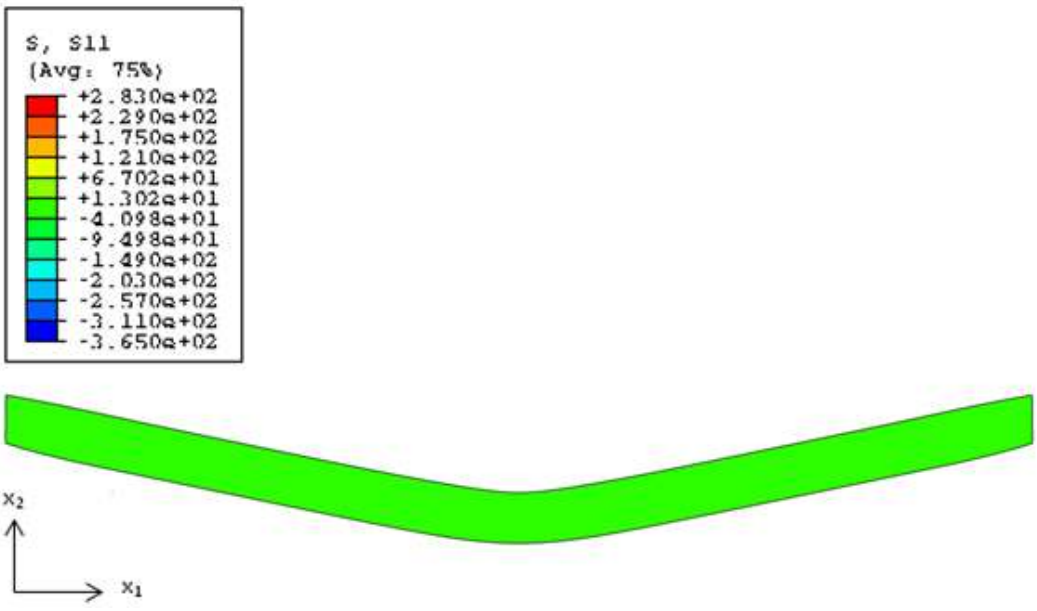

Fig. 3.11. Contour plot longitudinal stress (σ_{11}) at 17530 hours (approximately 2 years).

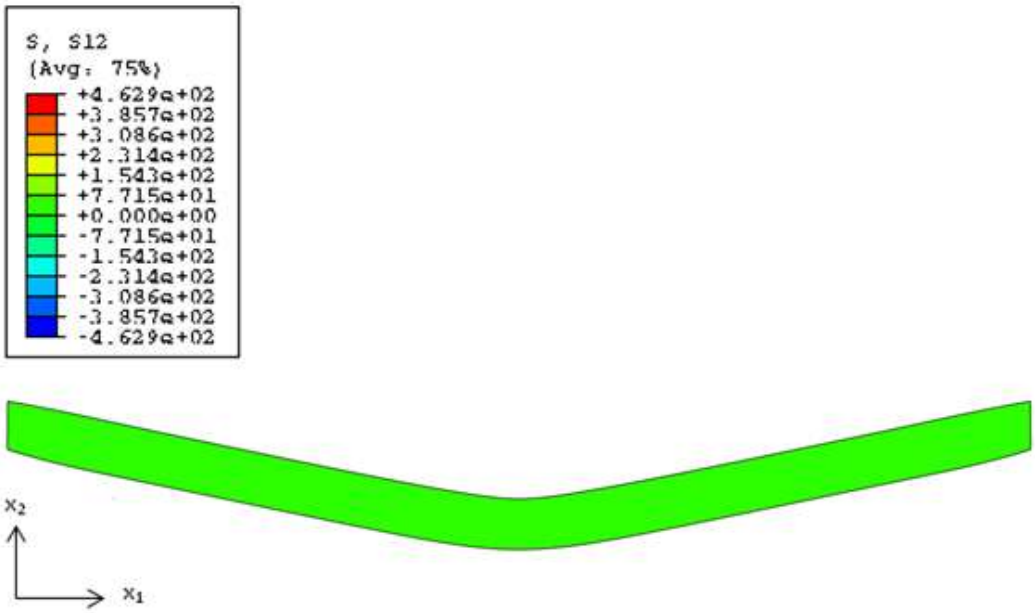

Fig. 3.12. Contour plot of shear stress (σ_{12}) at 17530 hours (approximately 2 years).

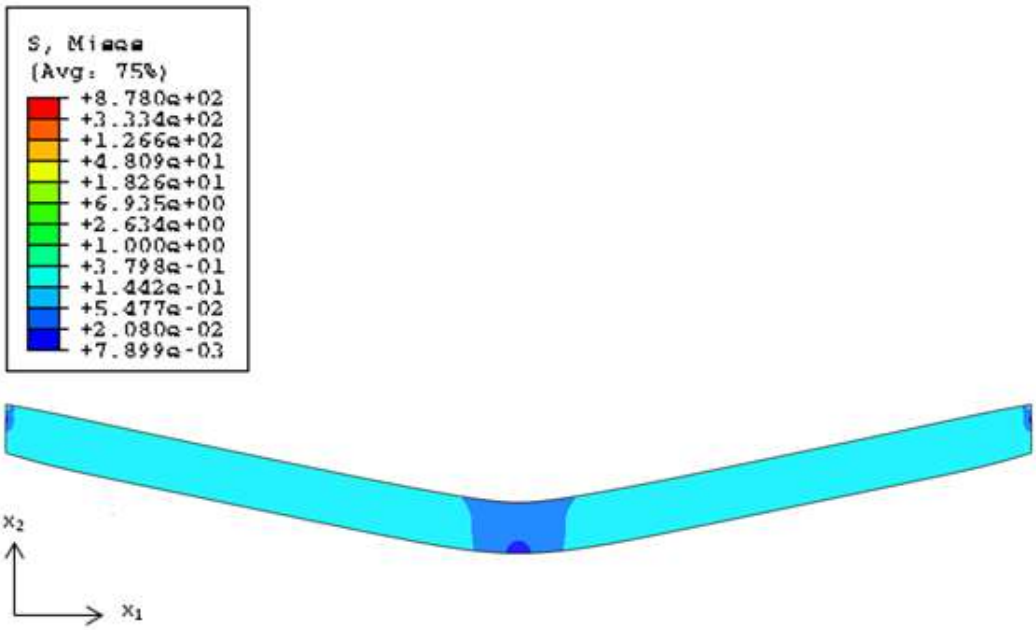

Fig. 3.13. Contour plot of the von Mises stress at 17530 hours (approximately 2 years).

In Fig. 3.14, the longitudinal strain (ε_{11}) represents the ratio of the change in length in the x_1 axis to the total length of the body and is due to the bending deformation at three different times. It is seen in Fig. 3.14.a, at an early time, the magnitude of the strains is very small, almost negligible in comparison the other two times. This strain is mainly due to the elastic response. As the time increases, the impact of the strain becomes more apparent. When comparing the strain in the sandwich beam with the aluminum skins to the sandwich beam with GR/E laminate skins, as time increases both sandwich systems experience an increase in strain which is expected. Both sandwich beams are experiencing compressive strain, which is negative at the top surface above the neutral axis. Below the neutral axis the beam experiences tension. At time 0.147 hours, the longitudinal strain is shown in a manner expected of longitudinal strain. During the times of 150.995 and 9663.676 hours, the longitudinal strain did not behave in the manner appropriate to strain in the core. Thus, an investigation on the extensional and compressive forces in the skins is performed. The net of the forces F_1 (bottom face) and F_2 (top face), should be approximately close to zero. It is noted that the foam core could also carry longitudinal stresses which result in forces in the longitudinal direction. However, the elastic modulus of the skins is much higher than that of the core resulting in negligible axial forces in the core. As the time increases, the sum of the forces at the top and bottom of the sandwich beam begins to increase as well. Equation 3.1 shows how the forces are calculated. The total length over time is derived based on the equation for strain which is shown in Eq. 3.2. The original length in compression decreases, whereas it increases in tension. So, a positive ΔL is added to the original

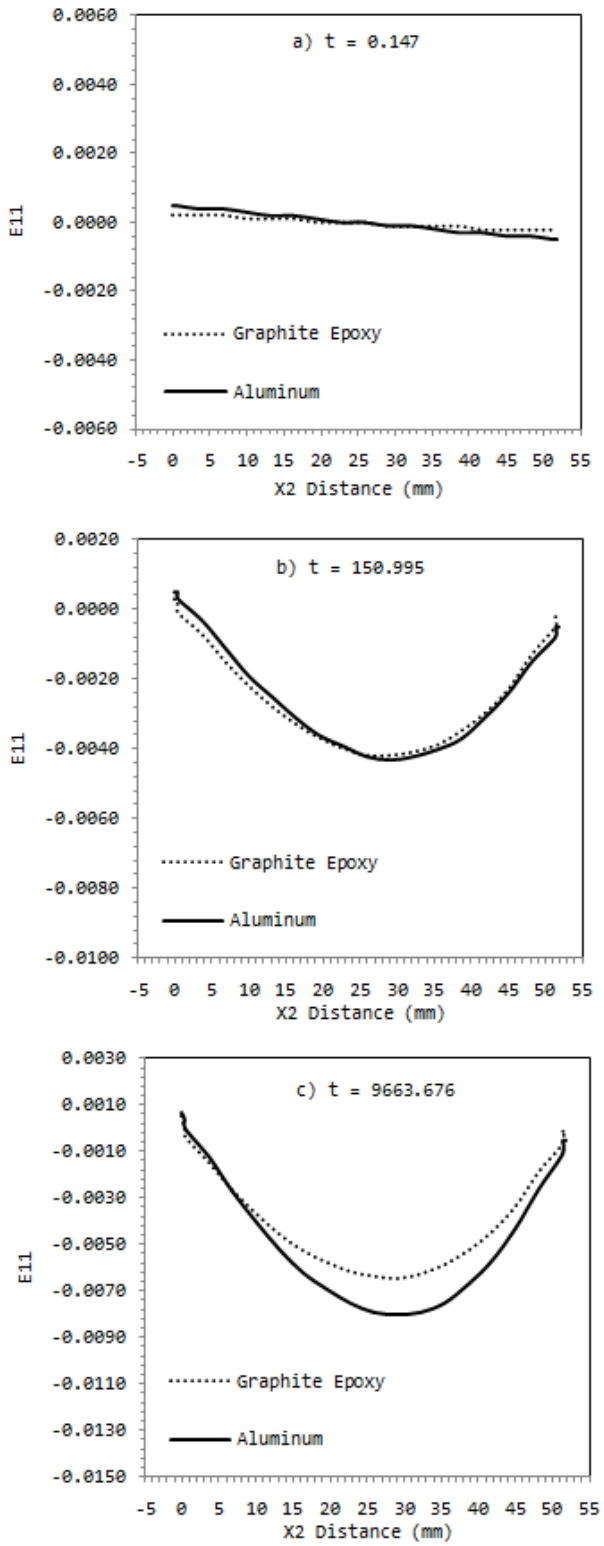

Fig. 3.14. Comparison of the longitudinal strain field at a distance of 83.3 mm from the midspan of the sandwich beam with aluminum of FRP as the skin material.

length in tension, where a negative ΔL is added to the original length in compression. When the forces for the top and bottom skins are summed, for times of 0.147, 150.995, and 9663.676 hours, they do not add up to zero. As a matter of fact, as the time increases the net force increases. The core experiences compression in order to compensate for the summed forces not being zero. In Table 3.4, the values for F_1 (bottom face) and F_2 (top face) are shown for all three of the times previously mentioned. The strain in the core increases as time increases and it is greater than the strain in the skins.

$$F = \frac{\sigma}{A} \quad \text{where,} \quad A = \text{cross - sectional area} \quad \text{and} \quad \sigma = \text{stress in skins} \tag{3.1}$$

$$\varepsilon = \frac{\Delta L}{L} \tag{3.2}$$

Table 3.4
Forces in the top and bottom skins of the sandwich beam

Time (hrs)		F_1, kN	F_2, kN	Net Force, kN
0.147	Aluminum	-81.18	81.45	0.3
	FRP	-81.27	81.53	0.3
150.995	Aluminum	-81.02	82.15	1.1
	FRP	-81.67	85.85	4.2
9663.676	Aluminum	-81.32	84.35	3.0
	FRP	-85.10	92.20	7.1

The shear strains (ε_{12}) through the thickness of the beam are nearly constant with an increase in strain nearing the top of the beam as shown in Figure 3.15. At the times of 0.147 and 150.995 hours, the strains in the sandwich beam with aluminum and GR/E laminate skins are very close in value. The distinction appears at the time of 9663.676 hours, where the aluminum is experiencing higher compression strain through the core than the GR/E laminate. As time increases, the shear strain in the core appears to decrease as it nears the top of the beam. The decrease can be related to how the beam is displaced over time. The concentrated point load is constant and does not change with time. During the time-dependent responses the sandwich beam continuously deforms increasing its deflection, which results in higher tension and compression stresses (strains).

The transverse strains (ε_{22}) through the thickness of the beam are in compression through the core for the Original at 150.995 and 9663.676 hours. In GR/E the beam is in compression through the core at the bottom of the beam and in tension through the core at the top of the beam at 150.995 and 9663.676 hours This is shown in Figure 3.16.

The longitudinal stresses (σ_{11}) for the sandwich beam are shown in Figure 3.17. In the bottom skin, the longitudinal stress are positive or in tension. This is the exact opposite for the top skin, where the longitudinal stress is negative or in compression. The stress in the top and bottom skins should be relatively the same, just opposite in sign. By inspecting the plot, it can be clearly seen how the skins are subjected to most of the stress. In the core, the longitudinal stress is fairly constant and significantly smaller than that of the skins. As time increases, the longitudinal stress near the bottom skin

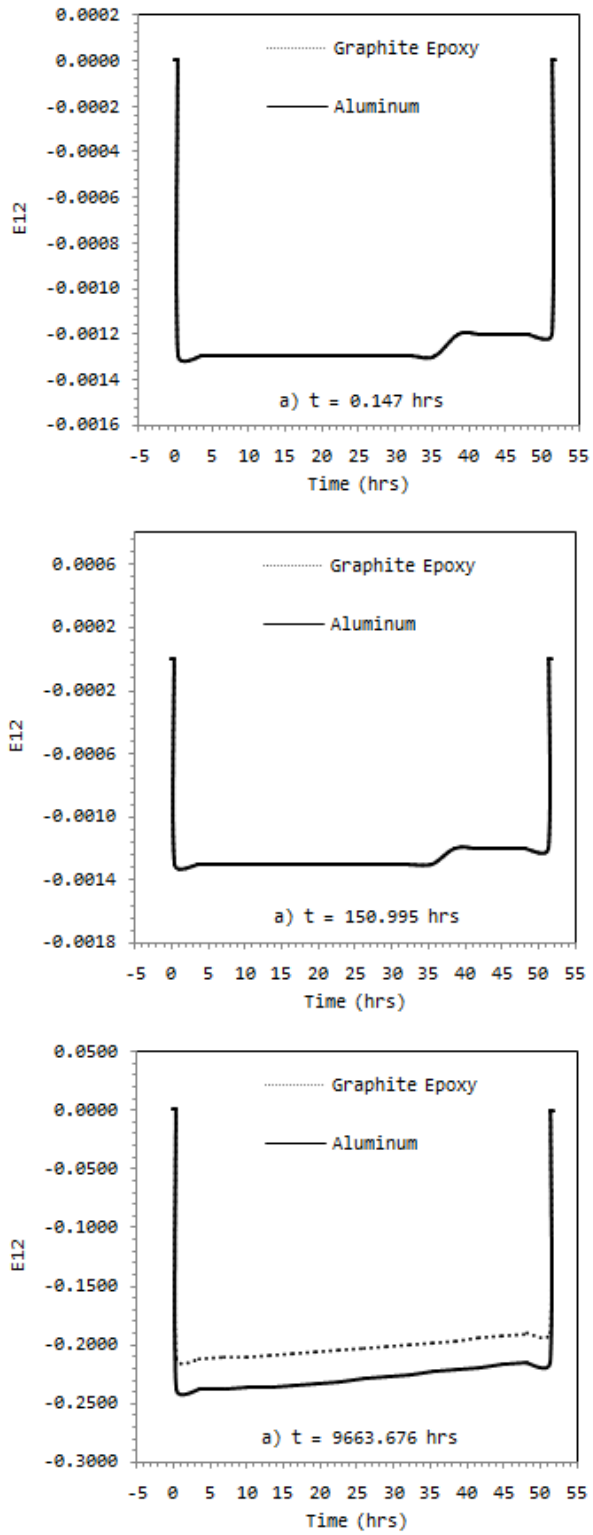

Fig. 3.15. Comparison of the shear strain field at a distance of 83.3 mm from the midspan of the sandwich beam with aluminum of FRP as the skin material.

(tension) becomes larger than the stress at the top (compression) as to maintain equilibrium condition during the creep deformation. The balance between the tension and compression begins to disappear as the stress in the bottom becomes greater than the stress at the top. To maintain overall equilibrium condition, the core would experience higher compression stresses.

The shear stresses (σ_{12}) for the sandwich beam with each skin material is shown in Figure 3.18. As time increases, the shear stress near the bottom of the beam is larger than that at the top. The average shear stress is equal to the force divided by the cross-sectional area. It is considered an average because the exact shear stress distribution is not uniform. Since the study is transient (time-dependent), the sandwich system will experience increases in shear stress as time increase due to bending. During this process, the beam will experience a change in its original parameters (e.g. length, height, and width).

In general, it is observed that the sandwich beam with the aluminum skins experiences higher strains through the core than the beam with GR/E laminate skins. With the stresses, the observation is reversed where the GR/E laminate experiences higher stresses in the skins than the aluminum. As time increases the sandwich beams begin to experience increased deformation, stresses, and strains.

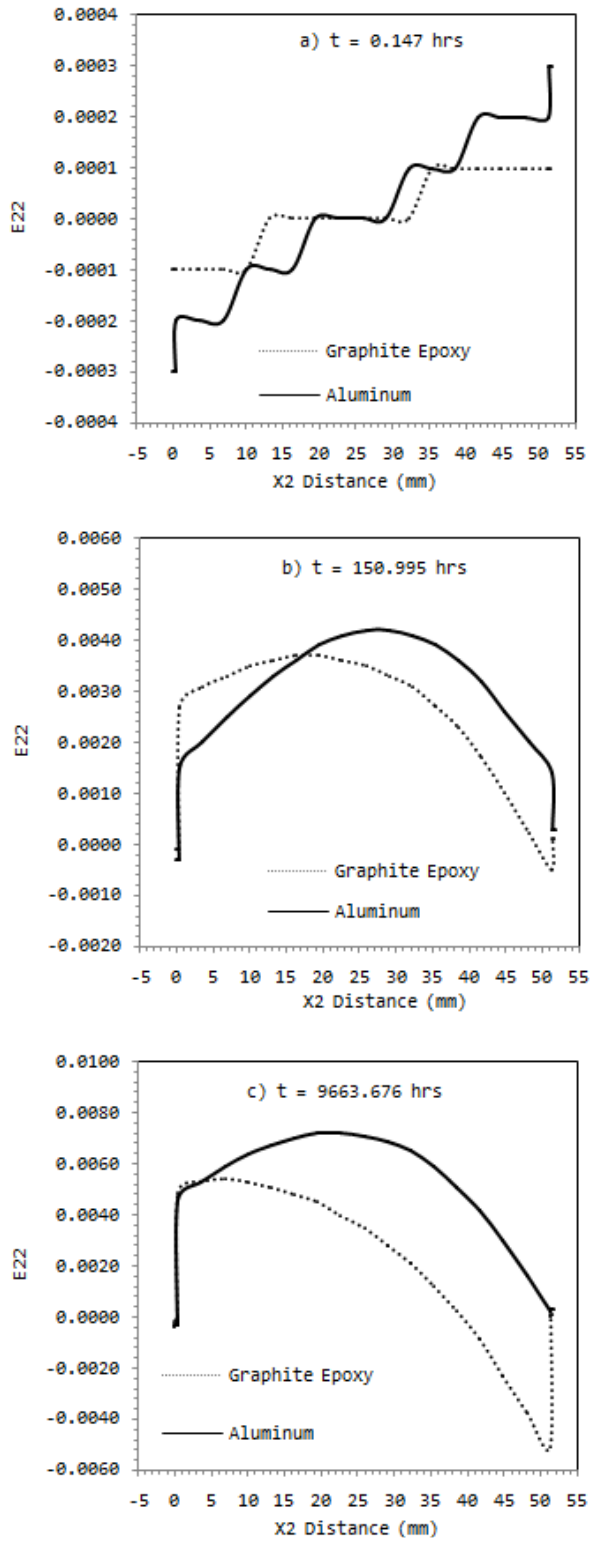

Fig. 3.16. Comparison of the transverse strain field at a distance of 83.3 mm from the midspan of the sandwich beam with aluminum of FRP as the skin material.

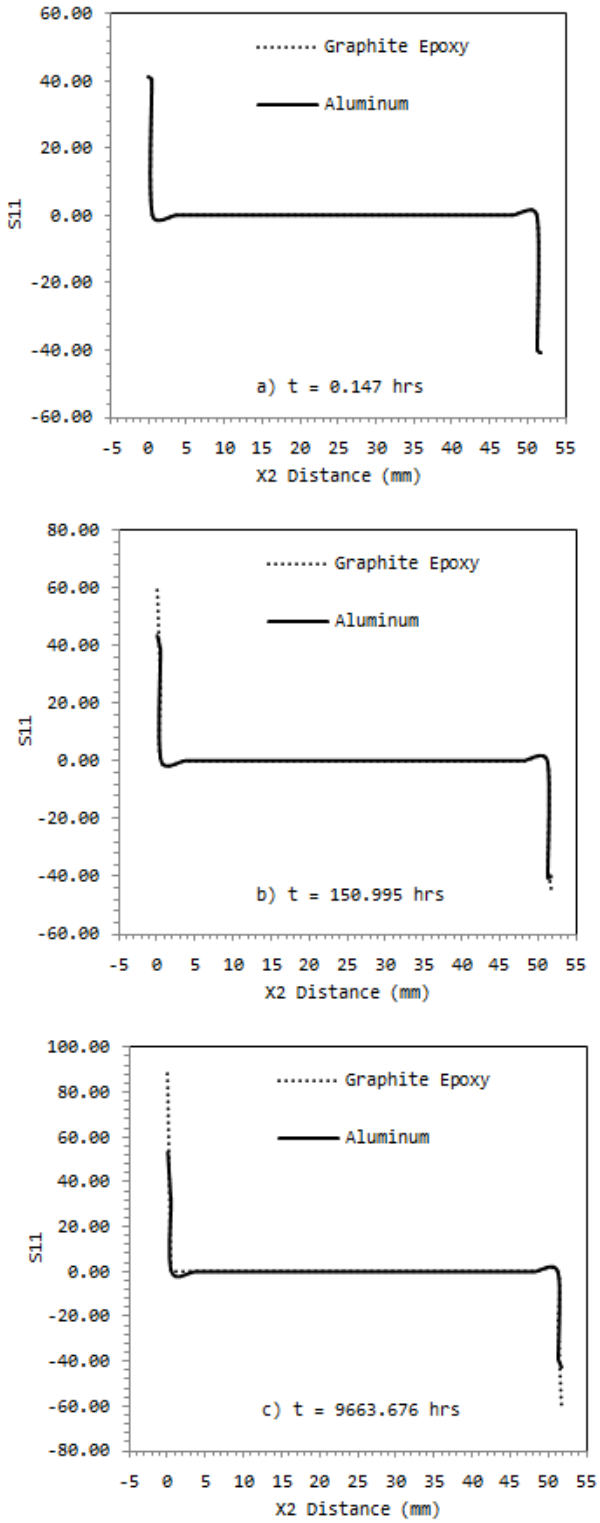

Fig. 3.17. Comparison of the longitudinal stress field at a distance of 83.3 mm from the midspan of the sandwich beam with aluminum of FRP as the skin material.

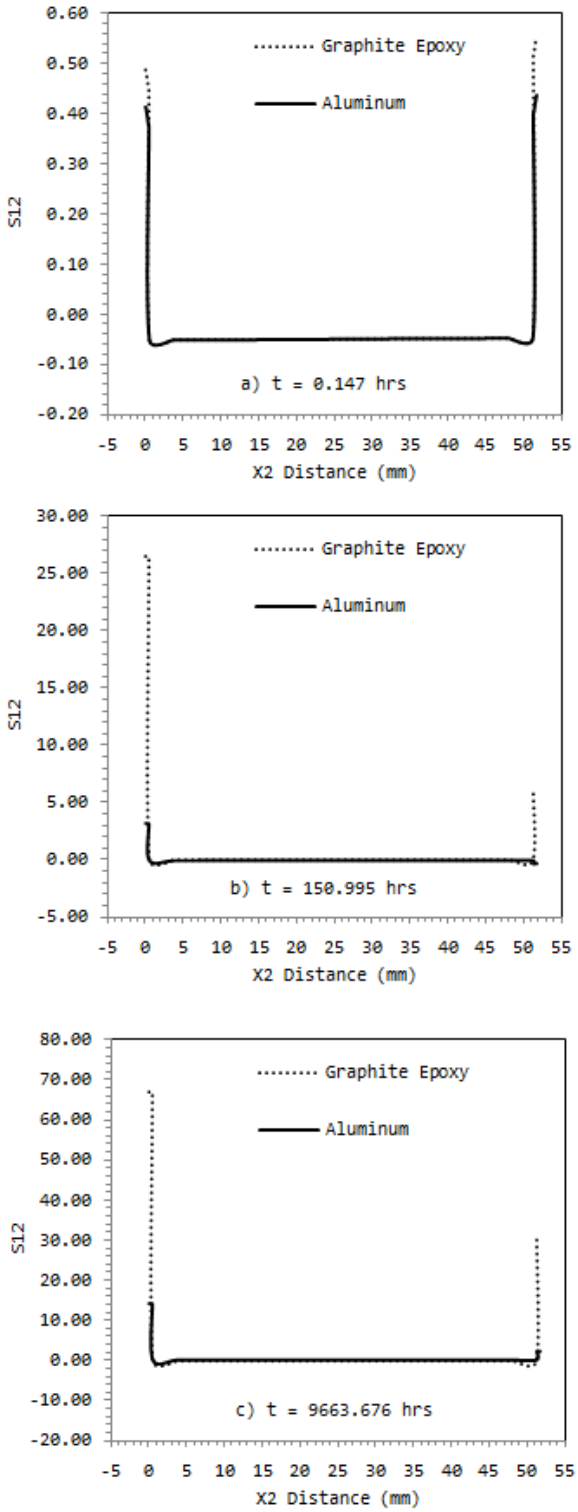

Fig. 3.18. Comparison of the shear stress field at a distance of 83.3 mm from the midspan of the sandwich beam with aluminum of FRP as the skin material.

CHAPTER IV

EFFECTS OF GEOMETRICAL AND MATERIAL PROPERTIES ON THE OVERALL VISCOELASTIC BEHAVIORS

Chapter IV presents parametric studies on understanding the effects of the core and skin thickness, the ratio of skin to core moduli, and the viscosity of the core foam on the overall viscoelastic responses of the sandwich beam. FE models are used to perform the study. The skins used for the reference sandwich beam are linear elastic aluminum and the core is linear viscoelastic polystyrene. Dimensions for the sandwich systems are 1000 mm long and 200 mm wide. The reference skins and core are 0.5 mm and 50.8 mm thick, respectively. All sandwich beams in the study are subjected to a 1000 N point load at the midspan of the beam. Sandwich beams with different skin to core ratios are generated by varying skin thickness and core thickness while keeping the total height of beam the same. Generally, in sandwich systems the skins are thin with high modulus while the core has a lower modulus and usually much thicker. The skin to core moduli ratios are varied using ratios equal to 0.1, 20, 35, and 100. In the viscosity study, parameters in the Prony series are multiplied by 2 or 0.5 to determine the effect of the viscosity of the foam core on the transient deformation in the sandwich beams. Furthermore, the effects of the thin adhesive layers, which are also assumed to be viscoelastic, on the time-dependent deformation are studied.

4.1 THE EFFECT OF THE RATIO OF SKIN TO CORE THICKNESS

A parametric study was performed on the ratio of skin to core thickness. Table 4.1 gives the thicknesses used for the skins and core. Figure 4.1 shows the creep deformation experienced by the sandwich beam when the thickness parameters are changed. Increasing the skin's thickness decreases the creep deformation significantly and this occurs only when the elastic skins are considered. The Original and T1 curves in Fig. 4.1 have considerably more creep deformation than T2. It is reasonable to assume that a sandwich beam with thicker skins will decrease the amount of creep deformation the beam will experience. This is only so if the relation between the skins and core is kept consistent in order to keep the strength in the skins as well as the rigidity created by the core. As the thickness of the aluminum skins is increased, the weight of the aluminum also increases. So, there is a range of thicknesses that would be optimal for the aluminum skins. Choosing a skin too small can result in failure and the beam experiencing high deformations. At the other end of the spectrum, choosing a skin too thick would increase the overall weight of the sandwich system.

Table 4.1
Sandwich beam skin and core thicknesses used in parametric study

	Skin Thickness, t_f (mm)	Core Thickness, t_c (mm)
Original	0.5	50.8
T1	2	47.8
T2	6	39.8

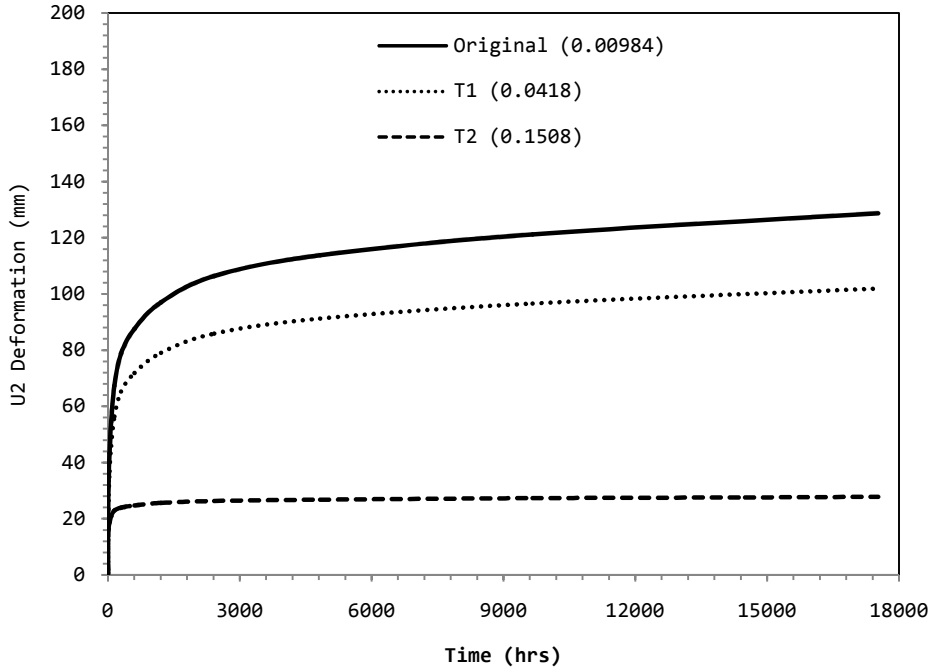

Fig. 4.1. Comparison of transverse creep deformation at midspan of sandwich beam for ratio of skin to core thickness study.

The longitudinal strain (ε_{11}) in Fig. 4.2, is the highest in the Original sandwich beam, this is reasonable considering it also experiences the largest creep deformation. The strains at 0.147 hours are relatively small and can be considered negligible in comparison to the other times. Longitudinal strain is defined as the ratio of the change in the length of a body to its original length. In later times as deformation increases, the core begins to experience compression throughout the entire thickness to compensate the high tension of the bottom skin. The cause for this occurrence is explained in Chapter III for the longitudinal strain of the aluminum and FRP skins. The Original sandwich beam is experiencing the most longitudinal strain and it also has the smallest skin to core ratio.

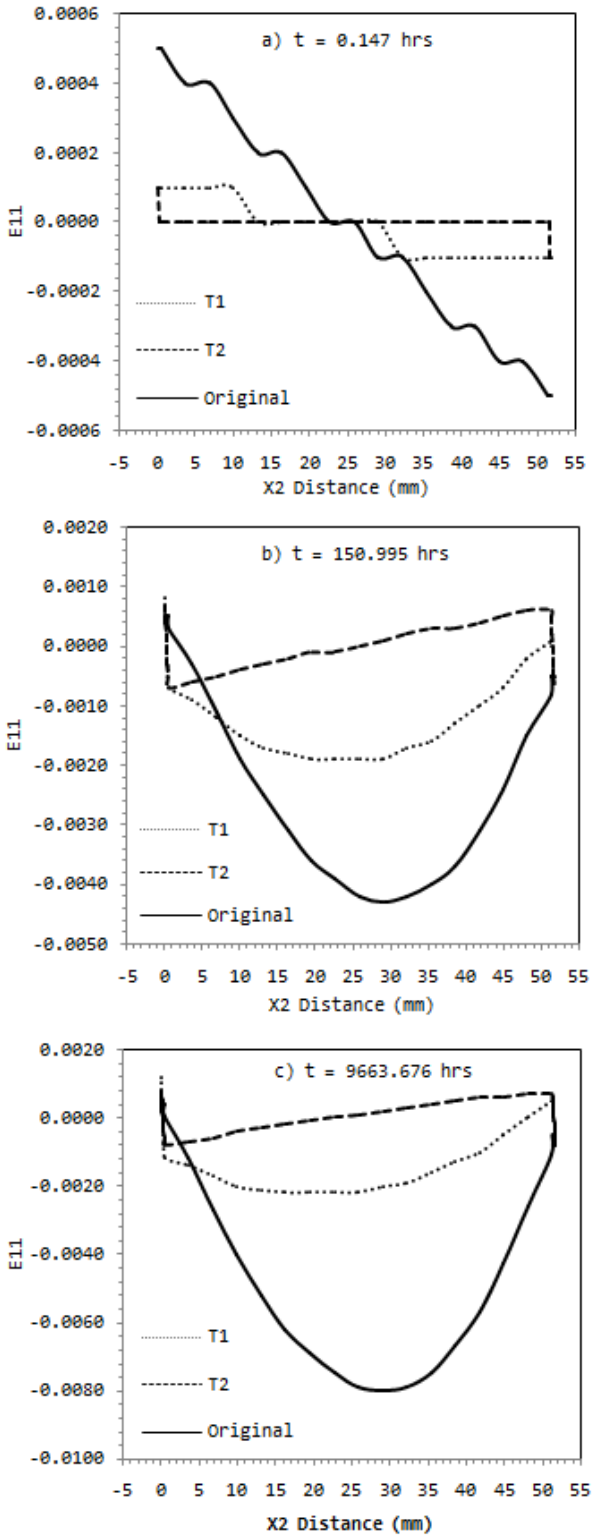

Fig. 4.2. Comparison of the longitudinal strain field at a distance of 83.3 mm from the midspan of the sandwich beam for ratio of skin to core thickness study.

The shear strain (ε_{12}) is shown in Fig. 4.3. It is produced by the shear stress. The Original sandwich system shows to have the greatest shear strain, while T2 and T1 show less shear strain, respectively. The skins in T1 and T2 are thicker than that of the Original beams, which means the skins can carry more loads which decreases the amount of strain the core experiences. There is a slight decrease in the shear strain in the top of the core and this can be linked to stress concentration. The effect of the thickness parameter on the transverse strain (ε_{22}) is shown in Fig. 4.4. Sandwich systems T1 and T2 are subjected to strains less to that of the Original.

The longitudinal stresses (σ_{11}) for the sandwich beam are shown in Figure 4.5. In the bottom skin, the longitudinal stress are positive or in tension. This is the exact opposite for the top skin, where the longitudinal stress is negative or in compression. The stress in the top and bottom skins should be relatively the same, just opposite in sign. By inspecting the plot, it can be clearly seen how the skins are subjected to most of

the stress. In the core, the longitudinal stress is fairly constant and significantly smaller than that of the skins. Due to the stress in the skins being much larger, the stresses in the core are insignificant. The balance between the tension and compression begins to disappear as the stress in the bottom becomes greater than the stress at the top. It is possible that the top of the beam is still experiencing the effects of the stress concentration. While the Original sandwich beam experiences the largest strain, it experiences the least amount of stress. This is opposite for T1 and T2, which experience lower strains and higher stresses than the Original. Sandwich systems T1 and T2 experience large jump discontinuities at the top and bottom interfaces which could trigger possible failure. The shear stresses (σ_{12}) for the sandwich beam with each skin material is shown in Figure 4.6. Sandwich beams T1 and T2 experience higher shear stresses than the Original sandwich beam. The high shear stresses at the interfaces could lead to delamination between the skin and the core.

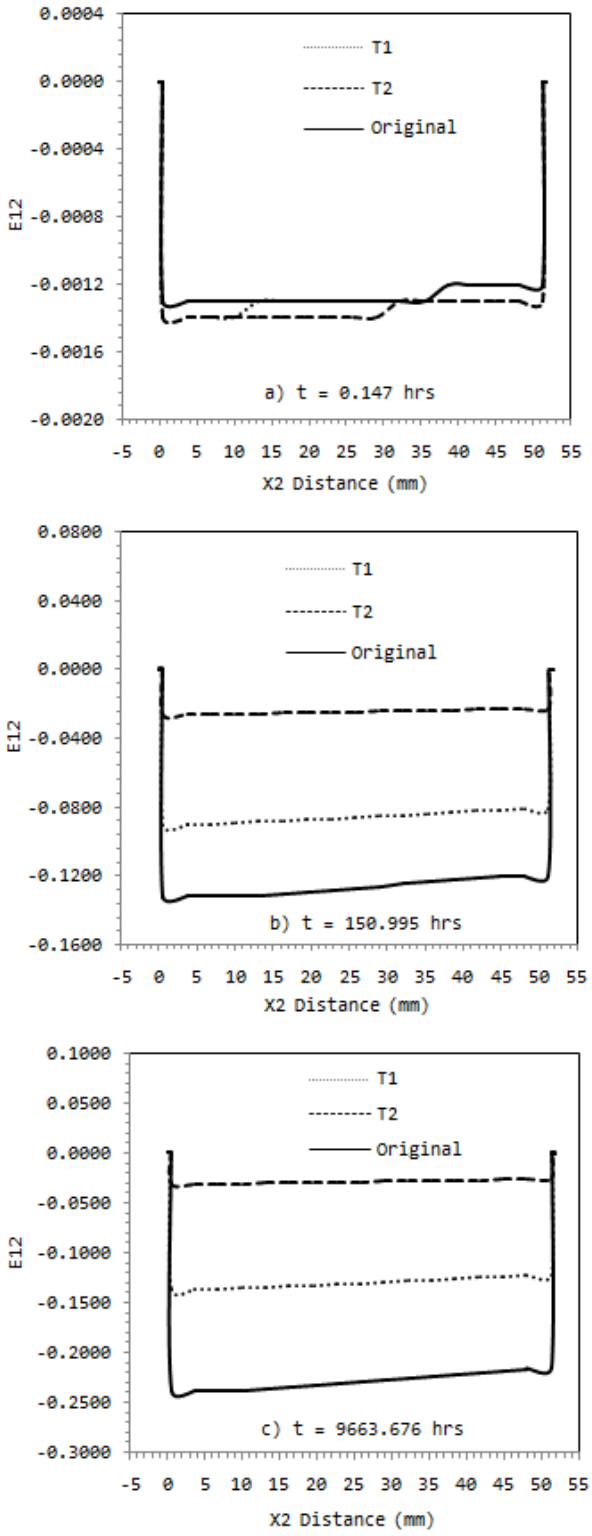

Fig. 4.3. Comparison of the shear strain field at 83.3 mm from the midspan of the sandwich beam for ratio of skin to core thickness study.

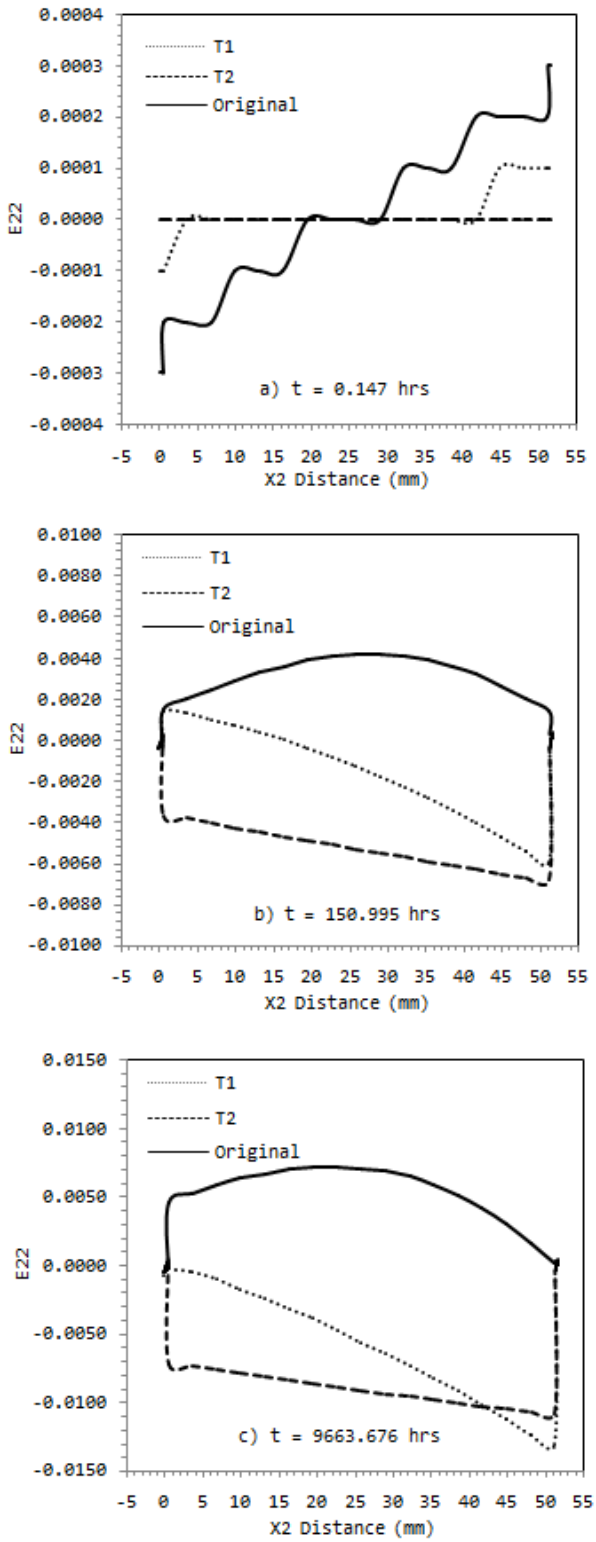

Fig. 4.4. Comparison of the transverse strain field at a distance of 83.3 mm from the midspan of the sandwich beam for ratio of skin to core thickness study.

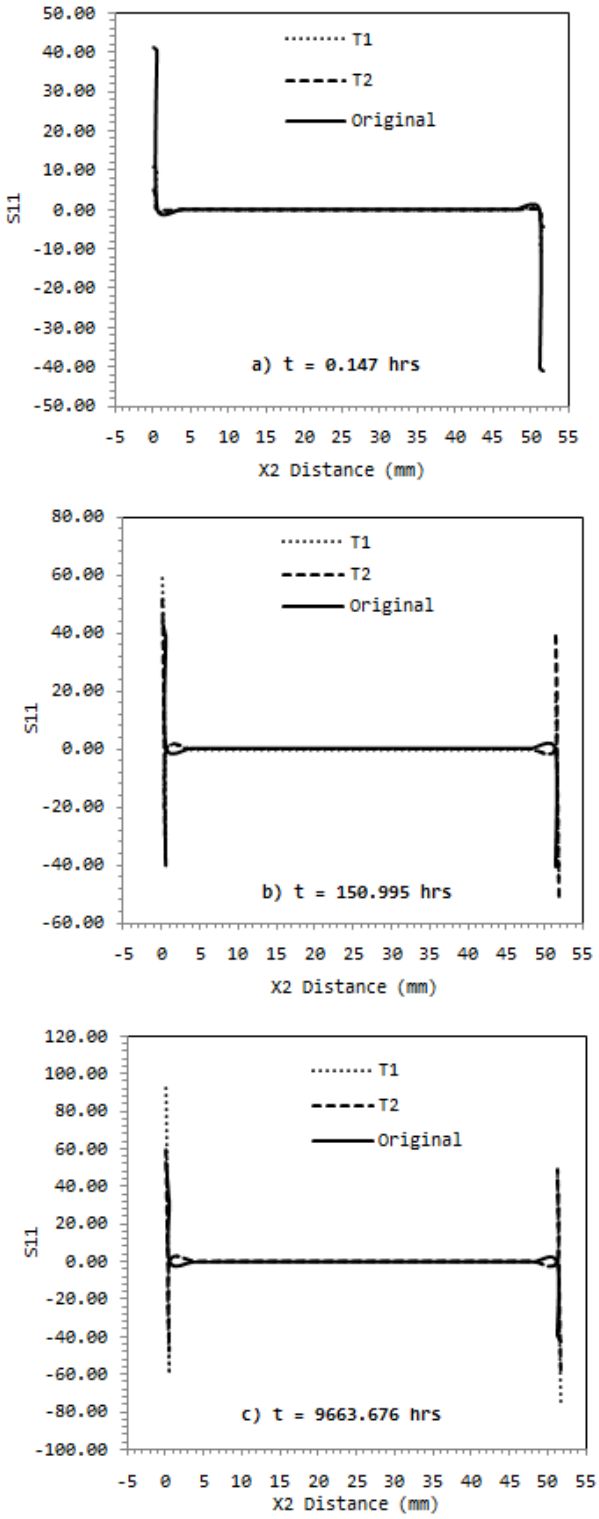

Fig. 4.5. Comparison of the longitudinal stress field at distance of 83.3 mm from the midspan of the sandwich beam for ratio of skin to core thickness study.

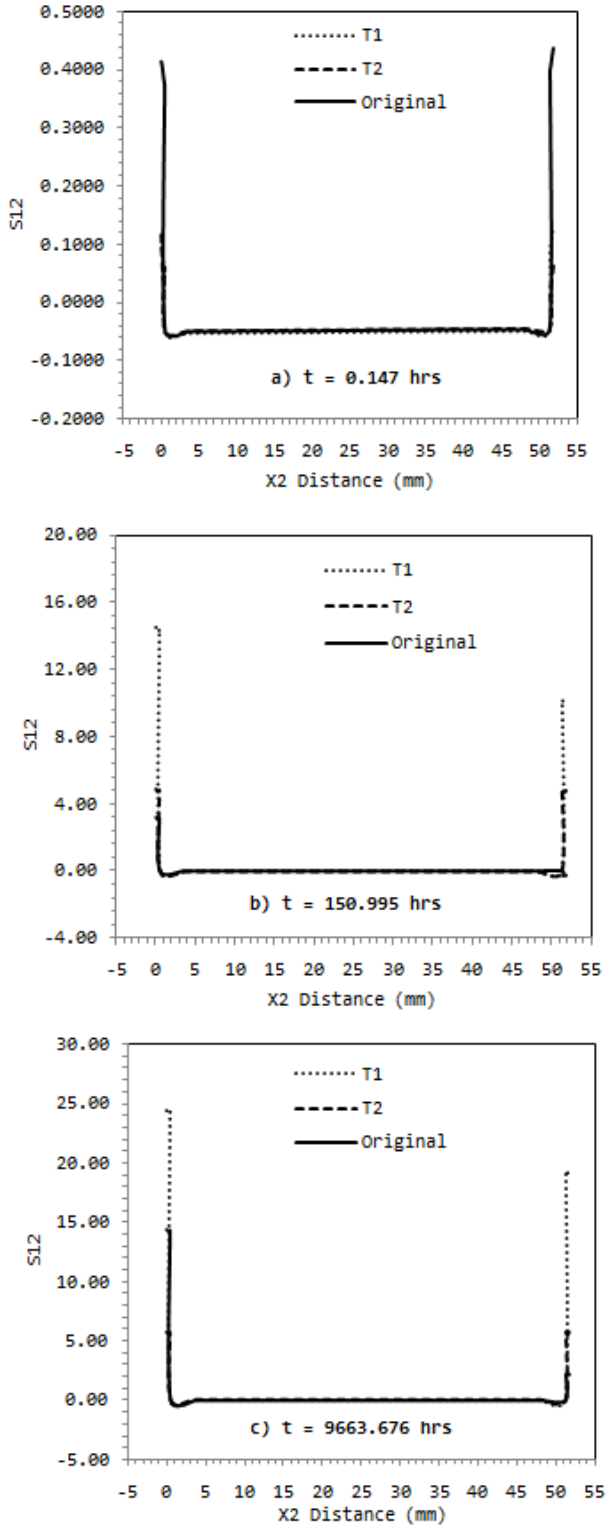

Fig. 4.6. Comparison of the shear stress field at distance of 83.3 mm from the midspan of the sandwich beam for ratio of skin to core thickness study.

4.2 THE EFFECT OF THE RATIO OF THE SKIN TO CORE MODULI

The effect of the ratio of the skin to core moduli was investigated. The modulus values used for this parametric study are given in Table 4.2. Figure 4.7 shows the creep deformation each parametric test is subjected to. For the sandwich system, the moduli of the skins and core are important to the performance. In M1, the ratio of the skin to core moduli is 0.1. When the ratio is less than 1, it means the skin modulus is less than the core modulus. The main purpose of the skin is to maintain the strength of the system and if the skin's modulus is less than the core's, an increase occurs in the creep deformation which is very apparent in the plot. It would be logical to assume the beam with the largest ratio would have the smallest deformation, but M2 has the smallest creep deformation. M3 has the largest ratio, and its core is weak in comparison to its large skin modulus. This is an ideal case, where $E_f >> E_c$. It is also seen from Fig. 4.7 that the overall deformation can be controlled by varying the modulus of the skins and core. There is a range of ratios of the skin to core moduli at which the overall deformation can be maintained. This gives flexibilities in choosing the various combinations of skin and core materials.

Table 4.2
Skin and core moduli values used for the parametric study

	Skin Modulus, E_f (MPa)	Core Modulus, E_c (MPa)
Original	70,000	2,000
M1	200	2,000
M2	200,000	10,000
M3	20,000	200

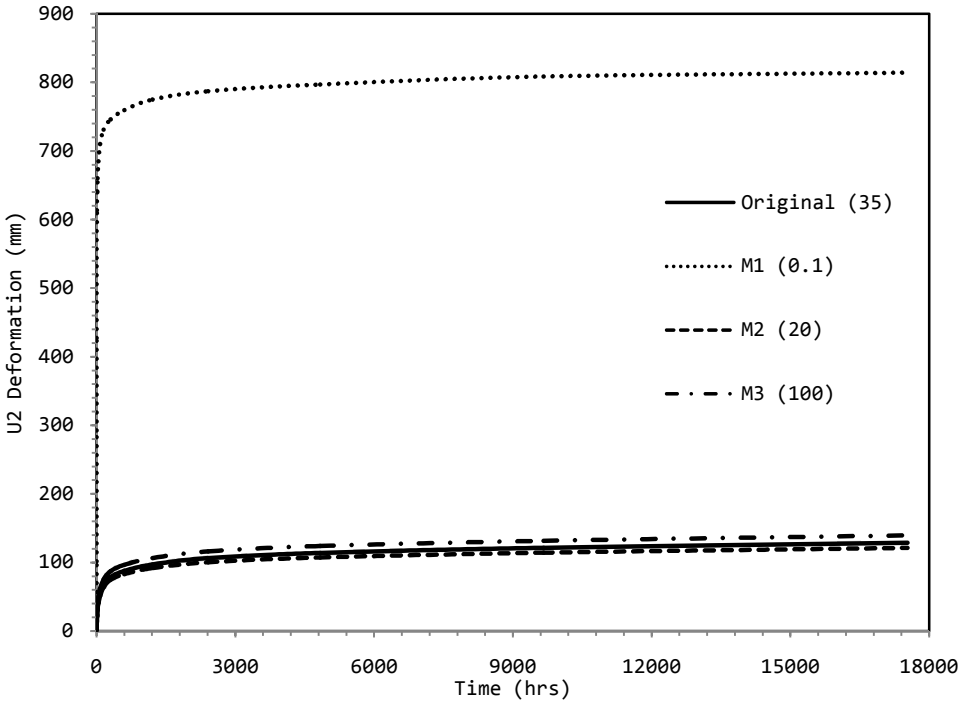

Fig. 4.7. Comparison of transverse creep deformation at midspan of sandwich beam for ratio of skin to core moduli study.

The longitudinal strain (ε_{11}) in Fig. 4.8, is the highest in the M1 beam, this is reasonable considering it also experiences the largest creep deformation. Longitudinal strain is defined as the ratio of the change in the length of a body to its original length. The strain is in tension in the bottom of the beam and in compression in the top part. The M1 sandwich beam is experiencing the most longitudinal strain and it also has the smallest skin to core moduli ratio. It is also the only beam where the skin modulus is less than the core modulus. It is noticed that as the modulus of the skin is increased, the strain in the core decreases. This occurs because the increased skin modulus also increases the

strength. As seen in Fig. 4.8, M2, M3, and the Original sandwich systems appear to have minimal longitudinal strain in comparison to M1.

The shear strain (ε_{12}) is shown in Fig. 4.9. The shear strain in the M1 sandwich beam is in tension, while M2, M3, and the Original systems are in compression. This would make sense considering the skin modulus is smaller and would have the opposite effect on shear strain. Since shear strain is related to the distortion in shape or skewing of a material, it is seen in Fig. 4.9 how the bottom part of the core is experiencing more compressive shear strain than the top. Overall, the shear strains for the sandwich systems are very close in value. This is even so for M1, which is close in value but in tension.

The effect of the moduli ratio on the transverse strain (ε_{22}) is shown in Fig. 4.10. The M1 sandwich beam has compressive strain through the bottom and extensional strain through the top. Transverse strain in M2, M3, and Original could be considered negligible in comparison to M1 and the original.

The longitudinal stresses (σ_{11}) for the sandwich beam are shown in Figure 4.11. In the bottom skin, the longitudinal stress is in tension for all the sandwich systems. In

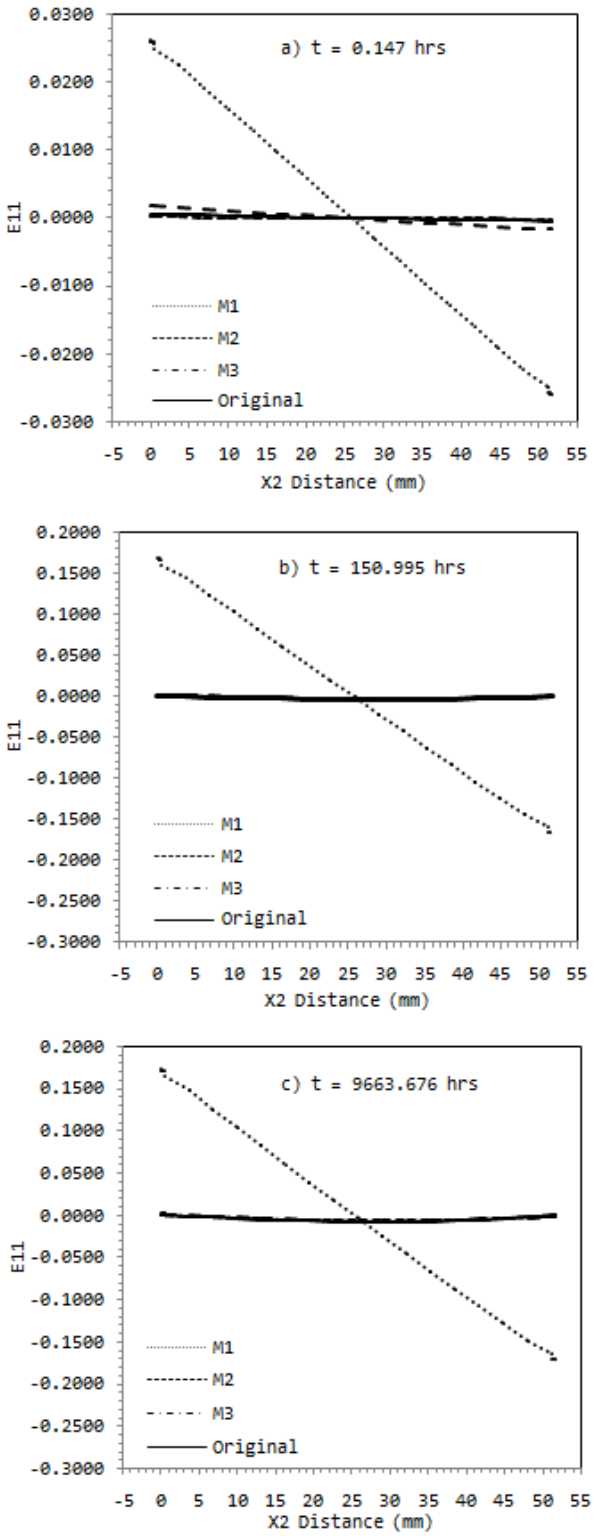

Fig. 4.8. Comparison of the longitudinal strain field at a distance of 83.3 mm from the midspan of the sandwich beam for ratio of skin to core moduli study.

the top skin, the longitudinal stress is in compression for all the sandwich systems and M2 experiences the most longitudinal stress. It also has the highest skin and core moduli. The stress in the top and bottom skins should be relatively the same, just opposite in sign. By inspecting the plot, it can be clearly seen how the skins are subjected to most of the stress. In the core, the longitudinal stress is fairly constant and significantly smaller than that of the skins. As time increases, the longitudinal stress near in the bottom skin becomes larger than the stress at the top. The balance between the tension and compression begins to disappear as the stress in the bottom becomes greater than the stress at the top. It is possible that the top of the beam is still experiencing the effects of the stress concentration. The shear stresses (σ_{12}) for the sandwich beam with each skin material is shown in Figure 4.12. M2 experiences the largest shear stress in tension and compression. It is also the sandwich beams with the largest skin modulus and largest core modulus. A stiffer core would result in higher shear stresses.

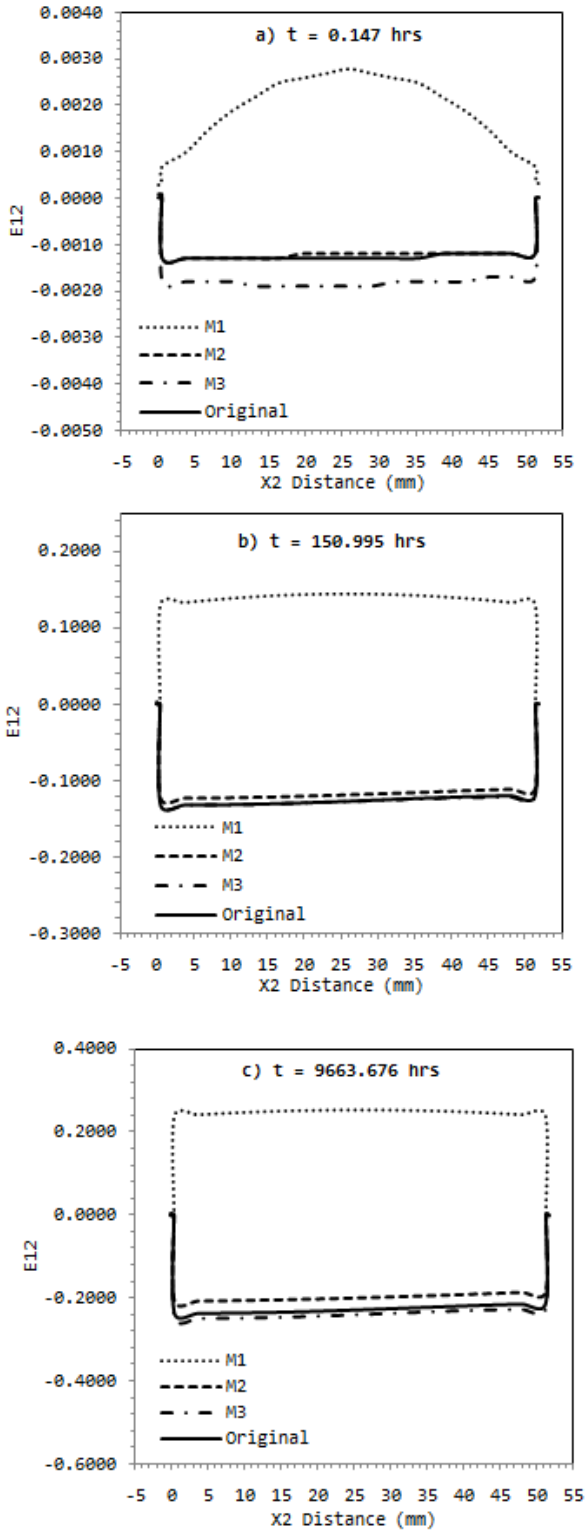

Fig. 4.9. Comparison of shear strain field at 83.3 mm from midspan of sandwich beam for ratio of skin to core moduli study.

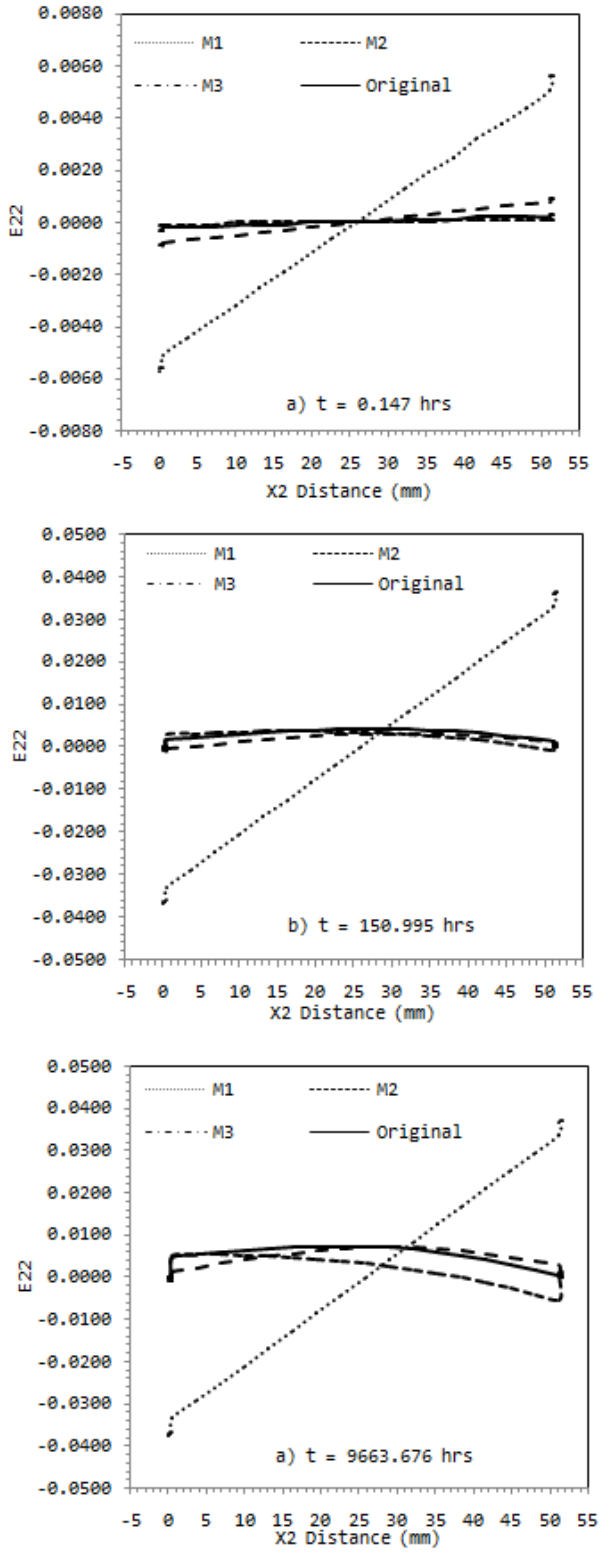

Fig. 4.10. Comparison of transverse strain field at a distance of 83.3 mm from the midspan of the sandwich beam for ratio of skin to core moduli study.

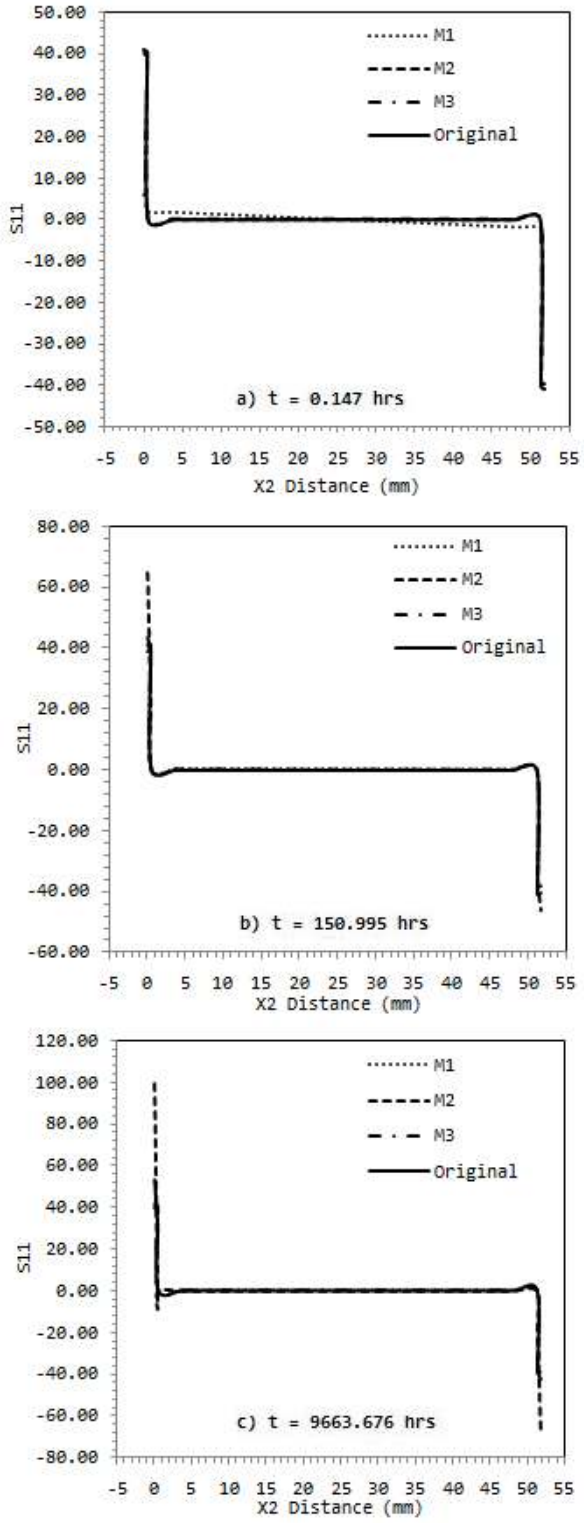

Fig. 4.11. Comparison of longitudinal stress field at a distance of 83.3 mm from the midspan of the sandwich beam for ratio of skin to core moduli study.

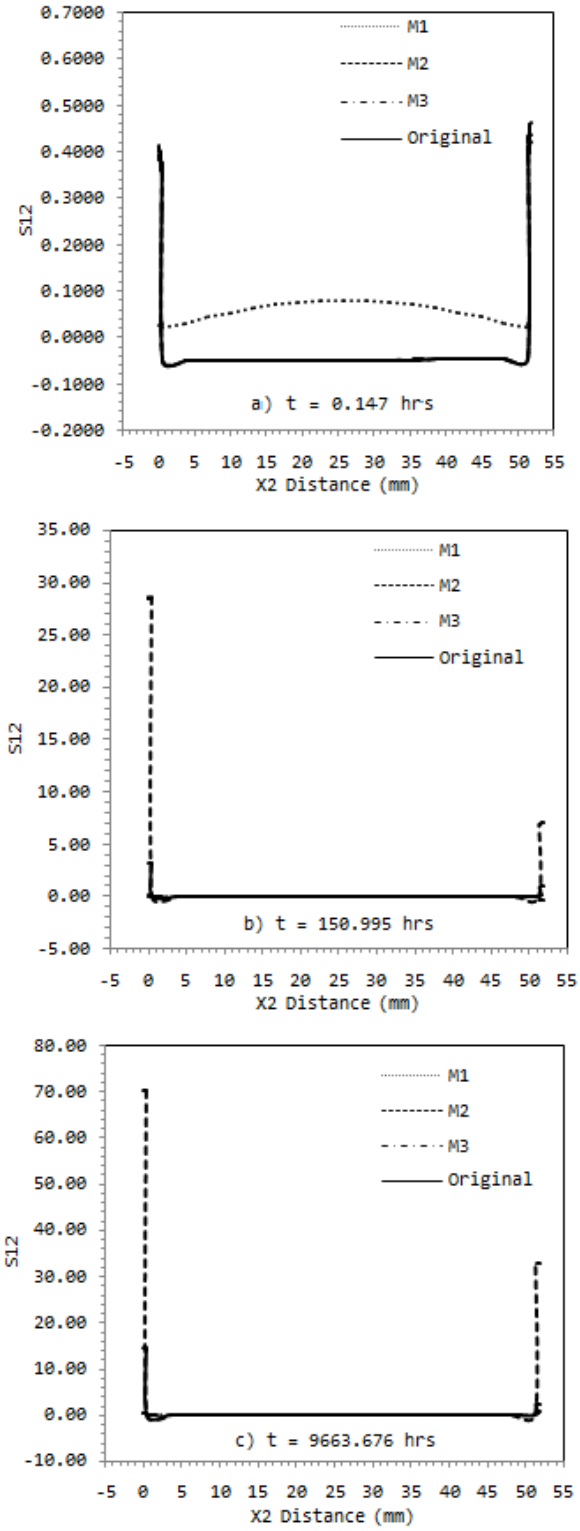

Fig. 4.12. Comparison of shear stress field at a distance of 83.3 mm from midspan of sandwich beam for ratio of skin to core moduli study.

4.3 THE EFFECT OF VISCOSITY IN VISCOELASTIC CORE

The effect of the viscosity of the core was investigated. In Table 4.3, it is shown which characteristics of the core's Prony series were tested. Viscosity is the measure of the resistance of a fluid against shear deformation. Even though the polystyrene core is not technically considered a "fluid", it is considered to be viscous because it flows to some extent in response to small shear stresses. The significance of this study is to determine which parameters within the Prony series used for the time-dependent core have the greatest effect on the overall deformation of the sandwich beam. The instantaneous modulus, series of exponentials, and the characteristic time are all multiplied by 0.5 and 2, representing a decrease and increase in the parameter. Through changing these parameters, it is determined under which conditions the sandwich beam will be more resistant to deformation.

Figure 4.13 shows the creep deformation for the viscosity according to the parameters changes in Table 4.3. It is clearly shown in the plot that V4 experiences the most creep deformation and V3 experiences the least deformation. In V4, the series of exponentials is multiplied by 2 and in V3 the series of exponentials is multiplied by 0.5. The series of exponentials represent the time-dependent part of the sandwich beam, which in this study is the polymer core. As time increases the compliance tends to increase as well, while the modulus relaxes with time.

Table 4.3
Changes to instantaneous modulus, Prony series, and characteristic time to determine the effect of viscosity

	Extensional Creep Compliance, MPa^{-1}
Original	$D(t) = D_0 + \sum_{n=1}^{N} D_n(1 - e^{-\frac{t}{\tau n}})$
V1	$D(t) = 0.5D_0 + A \quad where, \ A = \sum_{n=1}^{N} D_n(1 - e^{-\frac{t}{\tau n}})$
V2	$D(t) = 2D_0 + A \quad where, \ A = \sum_{n=1}^{N} D_n(1 - e^{-\frac{t}{\tau n}})$
V3	$D(t) = D_0 + 0.5A \quad where, \ A = \sum_{n=1}^{N} D_n(1 - e^{-\frac{t}{\tau n}})$
V4	$D(t) = D_0 + 2A \quad where, \ A = \sum_{n=1}^{N} D_n(1 - e^{-\frac{t}{\tau n}})$
V5	$D(t) = D_0 + \sum_{n=1}^{N} D_n(1 - e^{-\frac{t}{B}}) \quad where, \ B = 0.5\tau_n$
V6	$D(t) = D_0 + \sum_{n=1}^{N} D_n(1 - e^{-\frac{t}{B}}) \quad where, \ B = 2\tau_n$

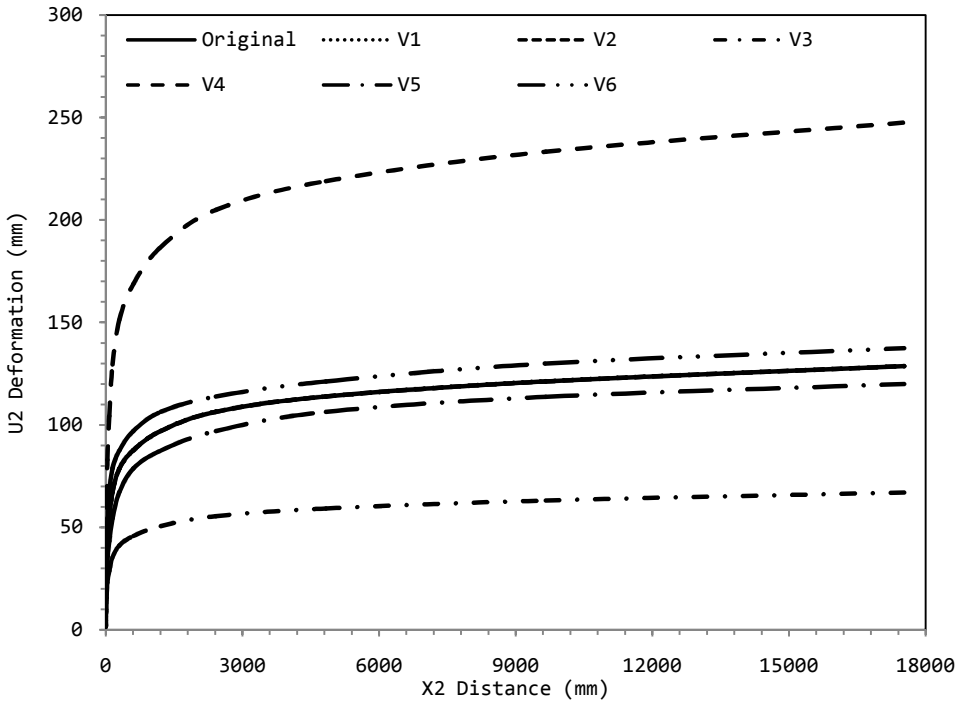

Fig. 4.13. Comparison of transverse creep deformation at midspan of sandwich beam for viscosity of the core study.

The longitudinal strain (ε_{11}) in Fig. 4.14, is the largest in the V4 sandwich beam, this is reasonable considering it also experiences the largest creep deformation. The strain is compression strain. At first the strain is fairly even at the time period of 0.147 hours and the strain through the bottom shows to be equal and opposite (in sign) to the strain through the top. The V4 sandwich beam experiences the largest longitudinal strain. V6 is the next lowest creep deformation and V5 is the next highest. In V5 and V6 the characteristic time was multiplied by 0.5 and 2, respectively. Longitudinal strain is defined as the ratio of the change in the length of a body to its original length. In later times, the core begins to experience compression throughout the entire thickness. The

cause for this occurrence is explained in Chapter III for the longitudinal strain of the aluminum and FRP skins.

The shear strain (ε_{12}) is shown in Fig. 4.15. The V4 sandwich system has the greatest shear strain. The effect of the thickness parameter on the transverse strain (ε_{22}) is shown in Fig. 4.16. The transverse strain is greater in the V4 and V5 beams.

The longitudinal stresses (σ_{11}) for the sandwich beam are shown in Figure 4.17. In the bottom skin, the longitudinal stress are positive or in tension. This is the exact opposite for the top skin, where the longitudinal stress is negative or in compression. The stress in the top and bottom skins should be relatively the same to maintain equilibrium condition. All of the viscosity study parameters have longitudinal stress plots that are very close in value. Since the shear effects in the core are dominant, it would make sense that V4 would experience more stress. The parameter change in the V4 beam is associated with the time-dependent core and basically represents the time-dependent creep compliance.

The shear stresses (σ_{12}) for the sandwich beam with each skin material is shown in Figure 4.18. The maximum shear stress is shown to occur in V2, and this reasonable since it parameter, the instantaneous modulus was doubled. All the other systems are very close in value according to the plots. Changing the instantaneous modulus, specifically increasing its value, will have a signification effect on the sandwich beam.

Based on the results in the plots, it can be seen that changing the instantaneous modulus parameter can have a great effect on the field variables of the sandwich beam.

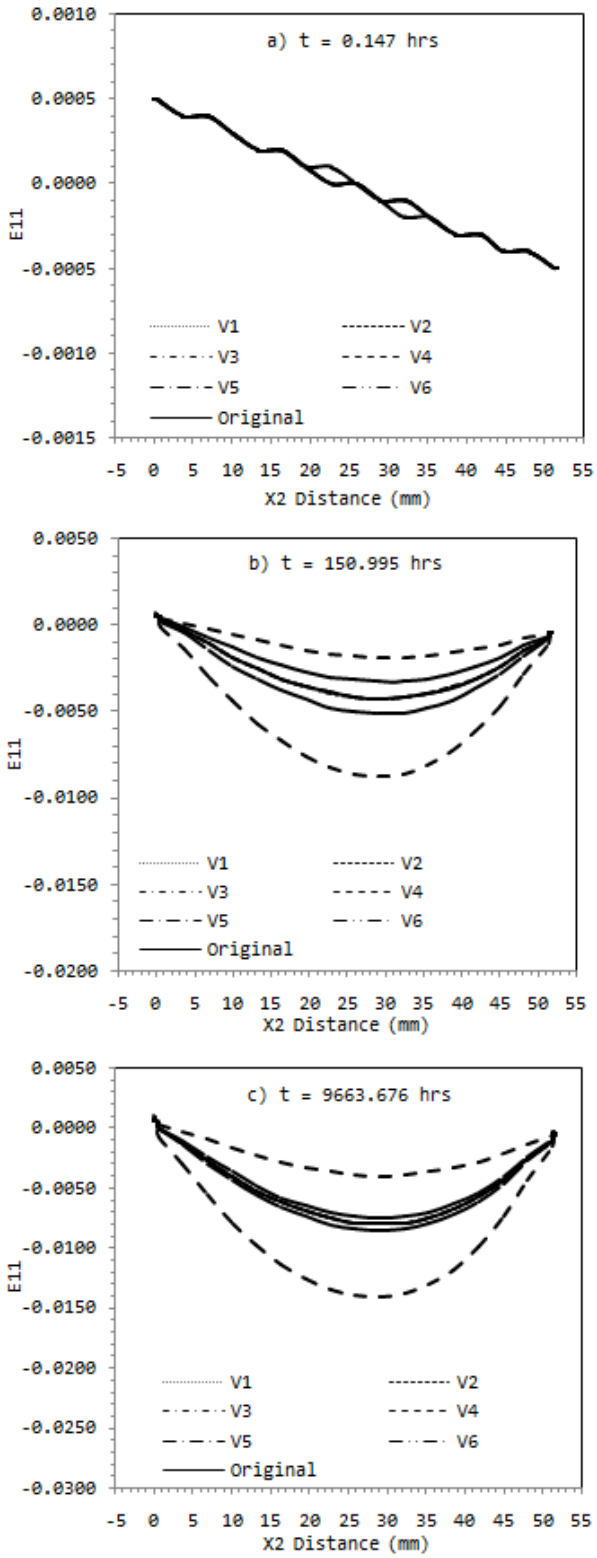

Fig. 4.14. Comparison of longitudinal strain field at a distance of 83.3 mm from the midspan of the sandwich beam for viscosity of the core study.

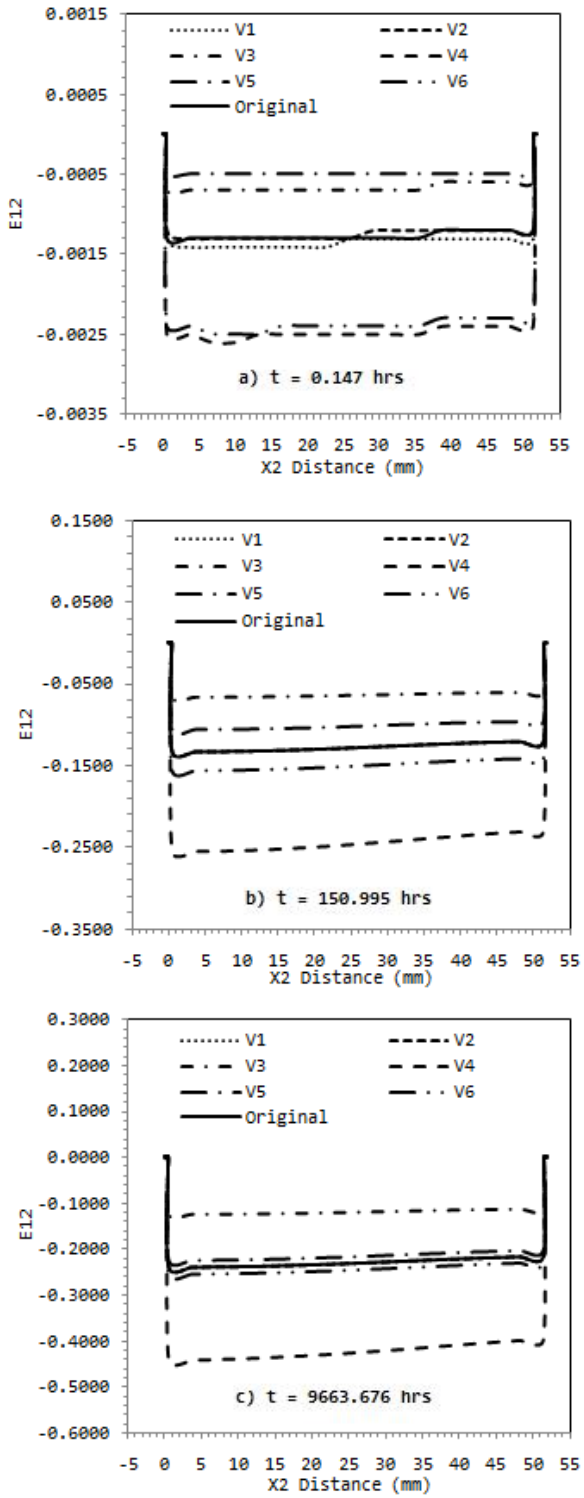

Fig. 4.15. Comparison of shear strain field at a distance of 83.3 mm from the midspan of the sandwich beam for viscosity of the core study.

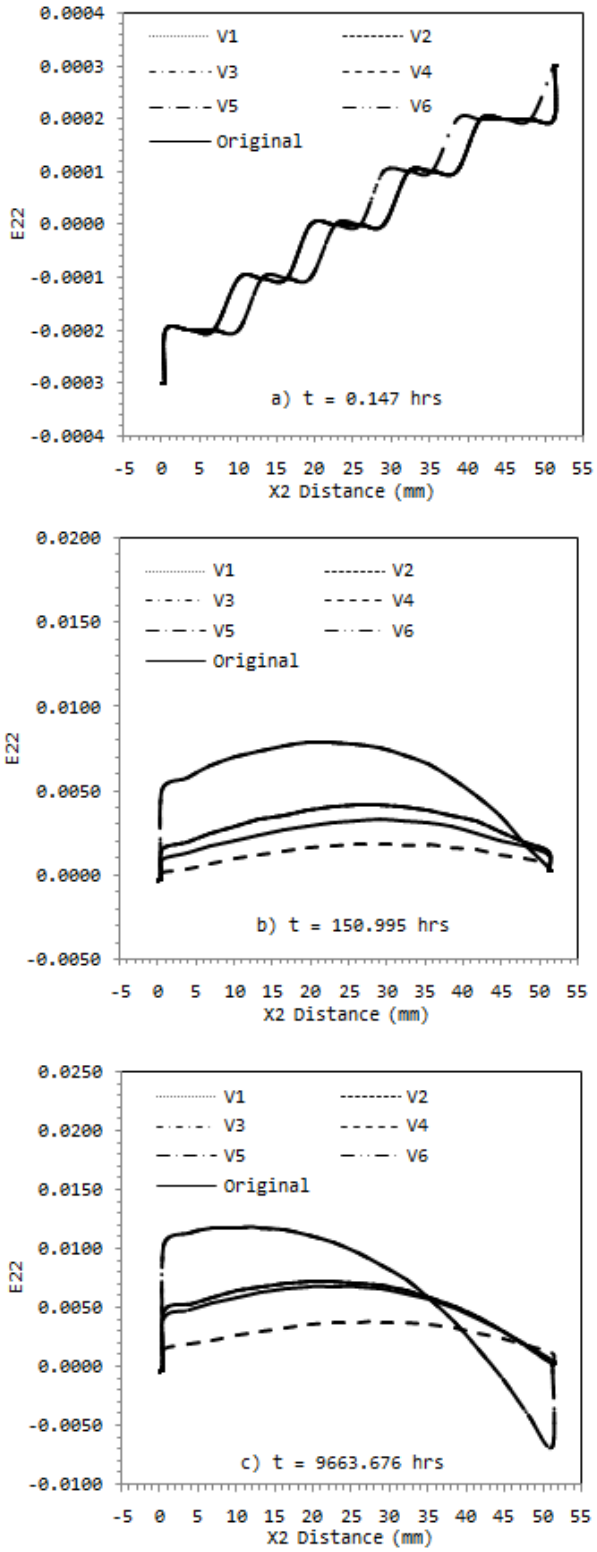

Fig. 4.16. Comparison of transverse strain at a distance of 83.3 mm from the midspan of the sandwich beam for viscosity of the core study.

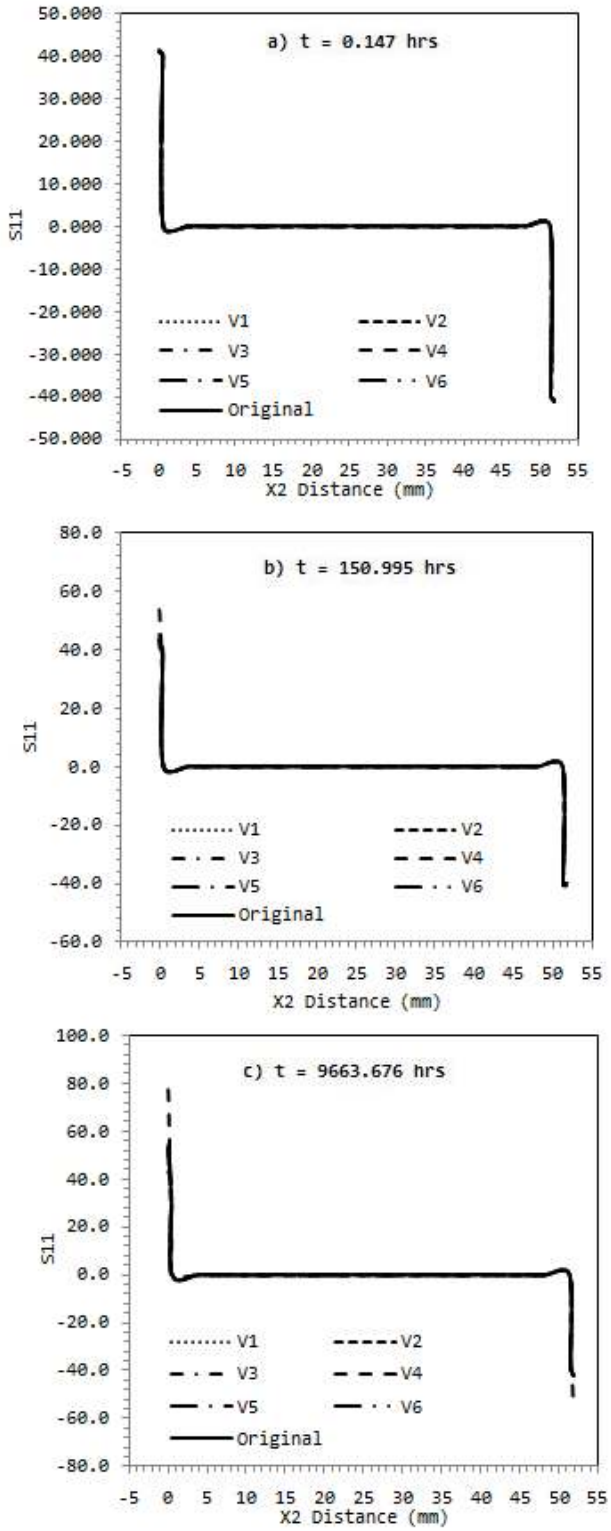

Fig. 4.17. Comparison of longitudinal stress field at a distance of 83.3 mm from the midspan of the sandwich beam for viscosity of the core study.

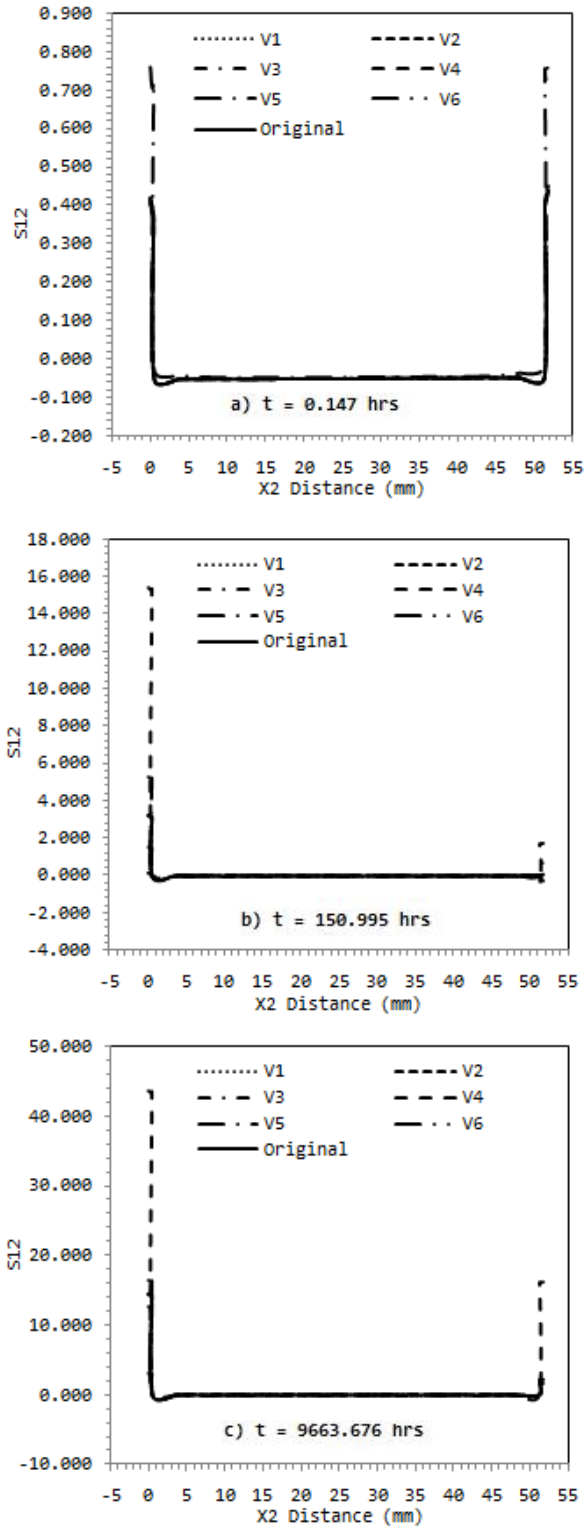

Fig. 4.18. Comparison of shear stress field at a distance of 83.3 mm from the midspan of the sandwich beam for viscosity of the core study.

4.4 THE EFFECT OF THE ADDITION OF ADHESIVE LAYERS

The effect of the addition of adhesive layers was investigated. Table 4.4 shows the time-dependent and elastic properties for the FM73 adhesive. Figure 4.19 shows the creep deformation at the midspan of the sandwich beam with and without adhesive layers. Adhesive layers are used to bond the skins and core, thus it is essential the adhesive layers are capable of transferring forces between the skins and the core. The purpose of this study is show that the thin layer of adhesive has no significant effect on the overall deformation of the sandwich system. Based on the time-dependent study, the beam with adhesive and the beam without adhesive have no significant change in their creep deformation. The percent difference for the sandwich systems at the maximum time of 17530 hours (approximately 2 years) is about 2%. In the case of this study, it is reasonable to assume the adhesive can be ignored. If this study included examining delamination of failure mechanisms, then the adhesive performance would become relevant.

Table 4.4
Prony series coefficients and elastic properties for FM73 adhesive (Muliana and Khan, 2008)

n	λ_n (s^{-1})	D_n x 10^{-6}, MPa^{-1}
1	1	21.0
2	10^{-1}	21.6
3	10^{-2}	11.8
4	10^{-3}	15.9
5	10^{-4}	21.6
6	10^{-5}	20.0
E = 2710 MPa ν = 0.35		

The characteristic time (λ_n) in FE model was implemented using hr^{-1}

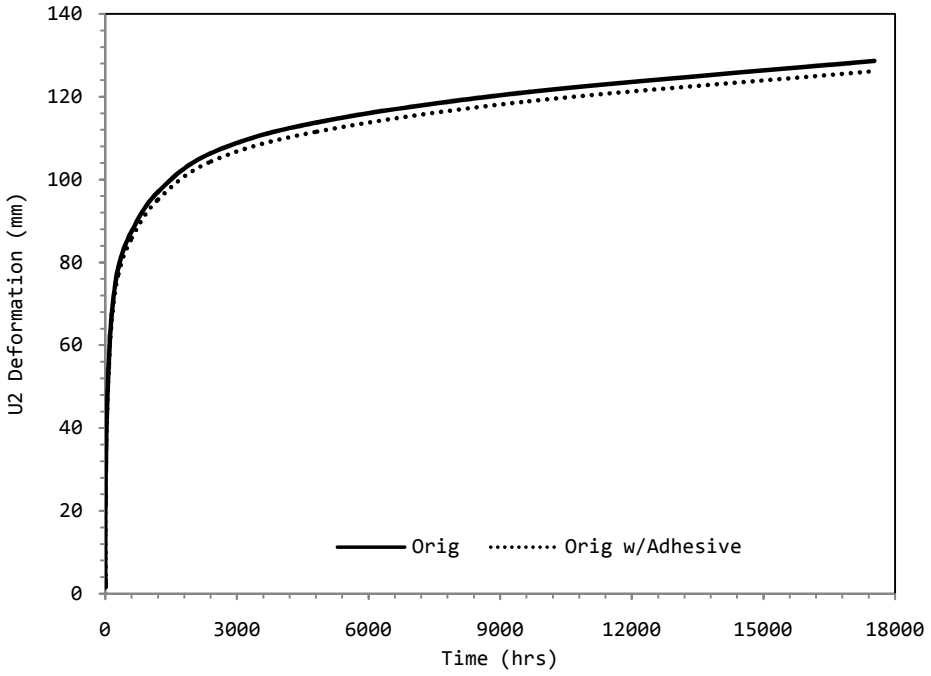

Fig. 4.19. Comparison of transverse creep deformation at midspan of sandwich beam for adhesive study.

The longitudinal strain (ε_{11}) for the sandwich beam with and without adhesive layers is shown in Fig. 4.20. It is very clear in the plot the beam with the adhesive experiences relatively the same strain as the beam without the adhesive. At first the strain is fairly even at the time period of less than an hour and the strain through the bottom shows to be equal and opposite (in sign) to the strain through the top. In later times, the core begins to experience compression throughout the entire thickness. The cause for this occurrence is explained in Chapter III for the longitudinal strain of the aluminum and FRP skins. The shear strain (ε_{12}) is shown in Fig. 4.21. Both sandwich systems have relatively the same shear strain. This correlates with the shear stress.

Having small shear stress values will also create smaller strain values. The effect of the thickness parameter on the transverse strain (ε_{22}) is shown in Fig. 4.22. The Original beam with adhesive and without adhesive both experience the same transverse strain which is expected since the adhesive is insignificant for this study.

The longitudinal stresses (σ_{11}) for the sandwich beam are shown in Figure 4.23. The stresses in the bottom skin layer show to be in tension and the stresses in the top layer show to be in compression. In the core, the longitudinal stress is fairly constant and significantly smaller than that of the skins. Due to the stress in the skins being much larger, the stresses in the core are insignificant. As time increases, the longitudinal stress near in the bottom skin becomes larger than the stress at the top. The balance between the tension and compression in magnitude appears to be close which is how the stress response if supposed to be as long as the sandwich system is functioning properly. The beam with the adhesive and the beam without the adhesive are very close in value, to where they look identical in the plot. This makes sense in that the adhesive is supposed to act in union with the sandwich system.

The shear stresses (σ_{12}) for the sandwich beam with each skin material is shown in Figure 4.24. The shear stress looks to be minimal at the top of the beam. Even though most of the shear stress is experienced in the bottom of the beam, the stress is still very small. At 9663.676 hours, the maximum strain in the bottom layer is around 15 MPa. The adhesive should have the capability to transfer the shear stresses between the skins and core.

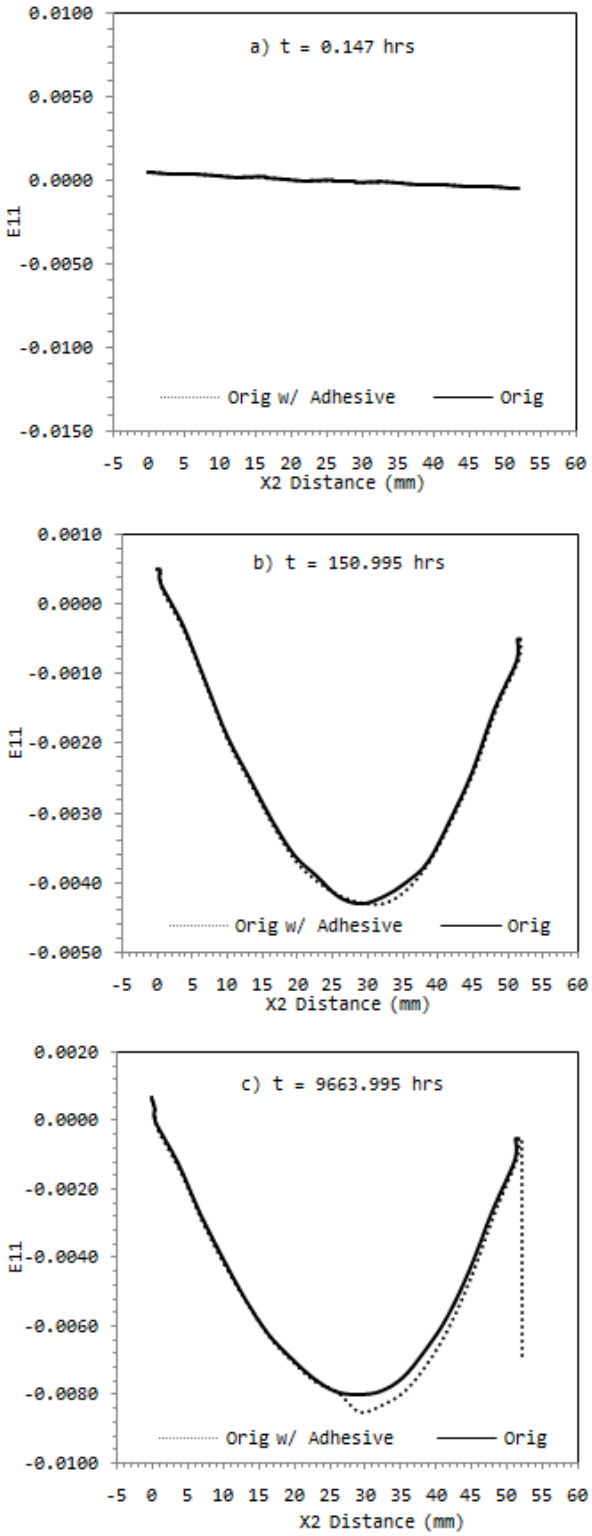

Fig. 4.20. Comparison of longitudinal strain field at a distance of 83.3 mm from the midspan of the sandwich beam for adhesive study.

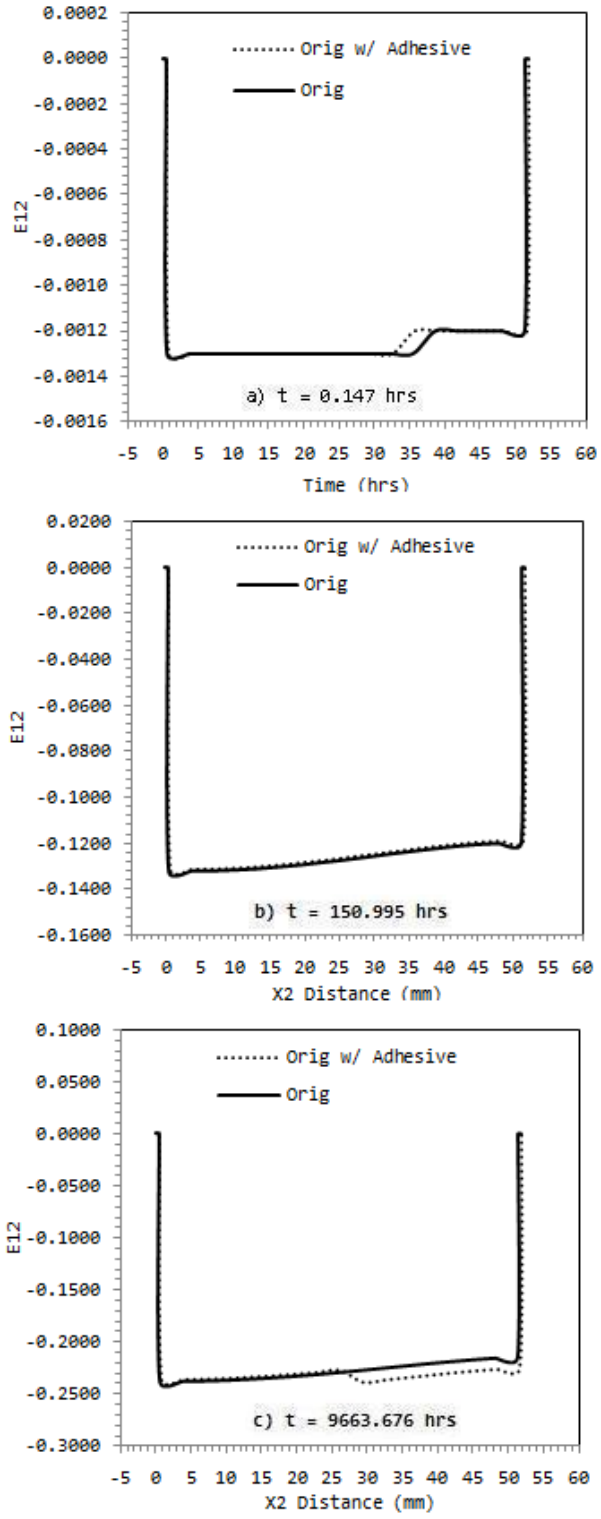

Fig. 4.21. Comparison of shear strain field at a distance of 83.3 mm from the midspan of the sandwich beam for adhesive study.

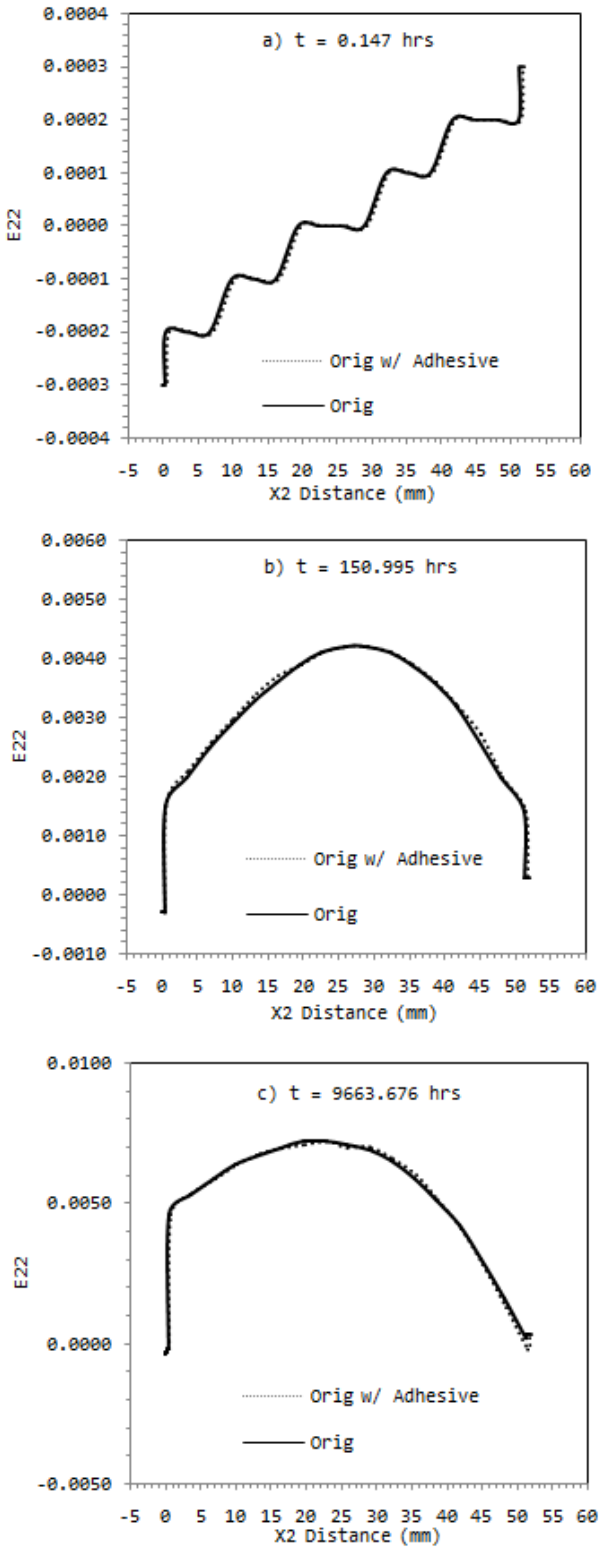

Fig. 4.22. Comparison of transverse strain field at a distance of 83.3 mm from the midspan of the sandwich beam for adhesive study.

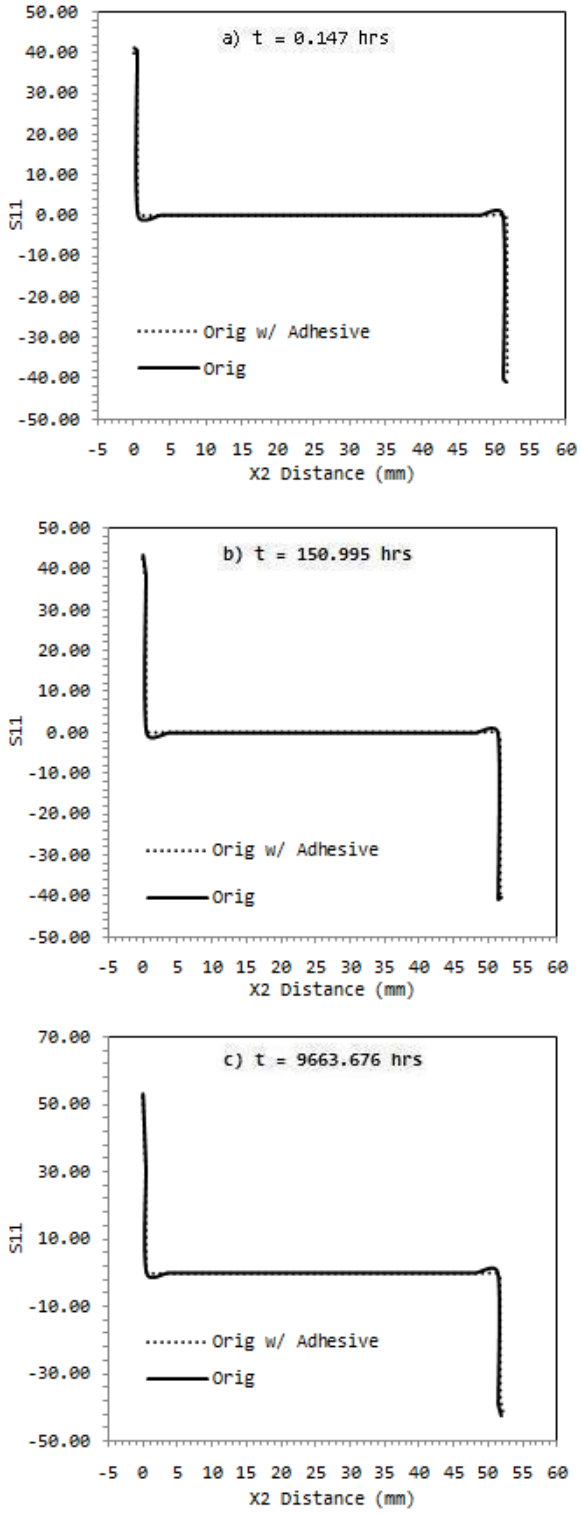

Fig. 4.23. Comparison of longitudinal stress field at a distance of 83.3 mm from the midspan of the sandwich beam for adhesive study.

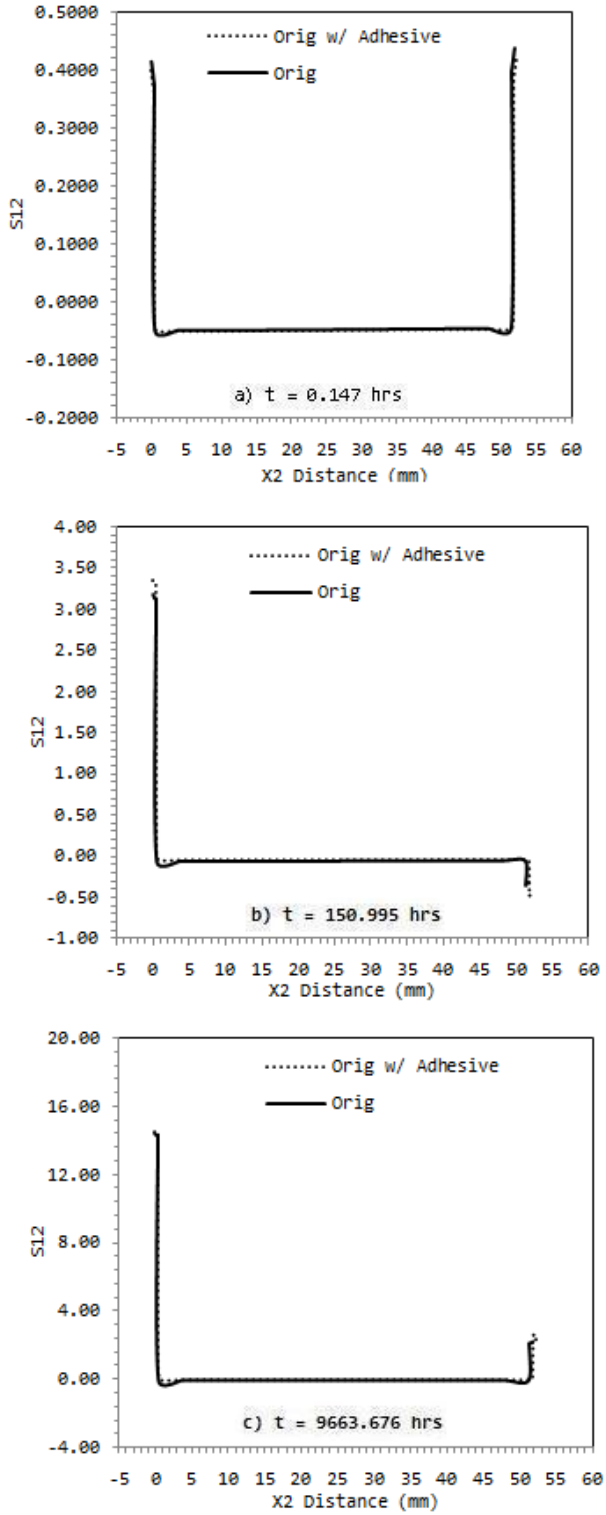

Fig. 4.24. Comparison of shear stress field at a distance of 83.3 mm from the midspan of the sandwich beam for adhesive study.

CHAPTER V

CONCLUSIONS AND FURTHER RESEARCH

5.1 CONCLUSIONS

The effect of a concentrated load applied over time on the deformation of viscoelastic sandwich composites, which are composed of linear isotropic or orthotropic fiber-reinforced skins and viscoelastic polymer, is analyzed. It is assumed that the skins are elastic (isotropic or orthotropic) and the core is linear viscoelastic, i.e., time-dependent. The governing equations of the deformation of viscoelastic materials are represented in differential form and hereditary integral form. A single integral constitutive equation is used to model linear viscoelastic materials by means of the Boltzmann superposition principle. The mechanical responses of viscoelastic materials such as stress relaxation function, creep compliance function, and characteristic creep and relaxation times are developed. To determine the stress or strain state in a viscoelastic material at any instant of time, the loading histories are included. A response to an arbitrary input loading is obtained by approximating the loading with multiple steps of input starting at different times. The uniaxial viscoelastic relation is generalized for the multiaxial 3D constitutive relations by separating the deviatoric and volumetric strain-stress relations (Joshi, 2008; Haj-Ali and Muliana, 2004).

Experimental data from literature is used to calibrate the Prony series of the polymer foam to be used in the analytical study. An analytical solution for viscoelastic deformation is performed to predict the overall performance of the studied sandwich

composites under three-point bending. The analytical solution to the deformation in a viscoelastic sandwich beam subjected to three-point bending is obtained from the strength of material approach with the use of the Correspondence Principle. The Correspondence Principle provides the means to convert the elastic linear solutions into solutions for linear viscoelastic problems by means of the Laplace transform provided certain conditions exist. The solutions are transformed back to the time domain solutions. 2D plane strain elements are used to analyze the overall time-dependent responses of a sandwich system subject to a concentrated point load. Results from the FE analysis are verified with the analytical models and available experimental data. A convergence study is used to analyze the size of the mesh on the overall response of the sandwich system and to ensure the results obtained are accurate as compared to the analytical solution. A comparison is made between a sandwich system with aluminum skins and a sandwich system with GR/E laminate skins to analyze the effect they have on the field variables, i.e., stress, strain, and displacement. The shear correction factor is discussed. In the FE analysis the shear stress is assumed to be uniform, therefore a value of one is assumed for k. The correction factor k is applied in order to account for the non-uniform distribution of shear stress and strain.

Parametric studies on the effects of the viscosity of the foam core, ratio of the skin and core thicknesses, ratio of the skin and core moduli, and adhesive layers on the overall performance of the sandwich beam are performed. Generally, as time increases the overall deformation in the sandwich structure increases. It is seen in the sandwich beams how changes to the geometrical and material properties can greatly affect the

strength, resistance to deformation, and the performance of the system. Adding layers of adhesive is found to be insignificant to the overall performance of the sandwich beam under bending in this study.

5.2 FURTHER RESEARCH

The current study on the analysis of sandwich beams having aluminum and FRP polymer skins and a polystyrene foam core is limited to the linear viscoelastic core. The study can be extended to include the moisture and temperature effect on the deformation. Sandwich beams are used for various applications in which the effects of the environment need to be included. The sandwich systems experience damage and failure and therefore the study can be extended to include these modes. The skins and core are susceptible to damage or failure related to delamination, core shear failure, compression failure, etc. All of the above parameters are important factors in the performance and life of a sandwich system.

REFERENCES

ABAQUS, Inc., 2007. Version 6.7 Documentation. Providence, RI.

Agosti, C.D., 2006. Viscoelastic characterization of rabbit nucleus pulposus tissue in torsional creep. Master Thesis. University of Pittsburgh.

Betten, J., 2005. Creep Mechanics. Springer-Verlag, Berlin.

Brancheriau, L., 2006. Influence of cross section dimensions on Timoshenko's shear factor – application to wooden beams in free-free flexural vibration. Annals of Forest Science 63, 319-321.

Chen, T., 2000. Determining a Prony series for a viscoelastic material from time varying strain data. NASA TM-2000-210123.

Christensen, R.M., 1982. Theory of Viscoelasticity. Academic Press, New York.

Ferry, J.D., 1980. Viscoelastic Properties of Polymers. Wiley, New York.

Flügge, W., 1975. Viscoelasticity. Springer-Verlag, Berlin.

Gnip, I.J., Vaitkus, S.I., Keršulis, V., 2005a. Analytical description of the creep of expanded polystyrene under compressive loading. Mechanics of Composite Materials 41 (4), 357-364.

Gnip, I.J., Keršulis, V.I., Vaitkus, S.I., S.A. Vėjelis, S., 2005b. Long-term prediction of creep strain of expanded polystyrene. Mechanics of Composite Materials 41 (6), 535-540.

Haj, R.M., Muliana, A.H., 2004. A multi-scale constitutive formulation for the nonlinear viscoelastic analysis of laminated composite materials and structures. International Journal of Solids and Structures. 41 (13), 3461-3490.

Hartsock, J.A., 1969. The design of urethane foam sandwich structures. Journal of Cellular Plastics 5 (3), 188-191.

Huang, J.S., Gibson, L.J., 1990. Creep of sandwich beams with polymer foam cores. Journal of Materials in Civil Engineering 2 (3), 171-182.

Joshi, N.P., 2008. Analyses of deformation in viscoelastic sandwich composites subject to moisture diffusion. M.S. Thesis. Texas A&M University.

Kim, J., Swanson, S.R., 2001. Design of sandwich structures for concentrated loading. Composite Structures. 52 (3-4), 365-373.

Lim, T.S., Lee, C.S., Lee, D.G., 2004. Failure modes of foam core sandwich beams under static and impact loads. Journal of Composite Materials 38 (18), 1639-1662.

Lukkassen, D., Meidell, A., 2007. Advanced Materials and Structures and their Fabrication Processes. HiN-book manuscript, Narvik University College.

Mase, G.E., 1970. Schaum's Outline of Theory and Problems of Continuum Mechanics. McGraw-Hill Companies, Inc., New York.

Muliana, A., Khan, K.A., 2008. A time-intergration algorithm for thermo-rheologically complex polymers. Computational Materials Science 41 (4), 576-588.

Nuñez, A.J., Marcovich, N.E., Aranguren, M.I., 2004. Analysis of the creep behavior of polypropylene-woodflour composites. Polymer Engineering and Science 44 (8), 1594-1603.

Partl, M.N., 2006. Linear viscoelastic behavior Boltzmann superposition principle. http://www.civeng.carleton.ca/courses/Grad/Partl2006S/3_LinViscoelastBoltzmann_.pdf

Qiao, P., Barbero, E.J., Davalos, J.F., 2000. On the linear viscoelasticity of thin-walled laminated composite beams. Journal of Composite Materials 34 (1), 39-68.

Raju, M., Reddy, C.R., Narasimha, S., Giridhar, G., 2006. Repair effectiveness studies on impact damaged sandwich composite constructions. Journal of Reinforced Plastics and Composites 25 (1), 5-16.

Rocca, S., Nanni, A., 2004. Design, fabrication and testing of low-profile composite bypass road panel: phase I. Missouri Department of Transportation. RDT 04-017.

Schniepp, T.J., 2002. Design manual development for a hybrid, FRP double-web beam and characterization of shear stiffness in FRP composite beams. M.S. Thesis, Virginia Polytechnic Institute and State University.

Scott, D.W., Lai, J.S., Zureick, A.H., 1995. Creep behavior of fiber-reinforced polymeric composites: a review of the technical literature. Journal of Reinforced Plastics and Composites 14 (6), 588-617.

Sharma, R.S., Raghupathy, V.P., 2008. A holistic approach to static design of sandwich beams with foam cores. Journal of Sandwich Structures and Materials 10 (5), 429-441.

Shaw, M.T., MacKnight, W.J., 2005. Introduction to Polymer Viscoelasticity. John Wiley and Sons, Inc., Hoboken.

Shenoi, R.A., Allen, H.G., Clark, S.D., 1997. Cyclic creep and creep-fatigue interaction in sandwich beams. Journal of Strain Analysis for Engineering Design 32 (3), 1-18.

Steeves, C.A., Fleck, N.A., 2004. Material selection in sandwich beam construction. Scripta Materialia 50 (10) 1335-1339.

Swanson, S.R., Kim, J., 2002. Optimization of sandwich beams for concentrated loads. Journal of Sandwich Structures and Materials 4 (3) 273-293.

Theocaris, P.S., 1964. Creep and relaxation contraction ratio of linear viscoelastic materials. Journal of Mechanics and Physics of Solids 12, 125-138.

Tschoegl, N.W., 1989. The Phenomenological Theory of Linear Viscoelastic Behavior. Springer-Verlag, Berlin.

Tschoegl, N.W., 1997. Time dependence in material properties: an overview. Mechanics of Time-Dependent Materials 1, 3-21.

Vinson, J.R., 2005. Sandwich structures: past, present and future. In: Thomen, O.T., Bozhevolnaya, E., Lyckegaard, A. (Eds.), Sandwich Structures 7: Advancing with Sandwich Structures and Materials, Proceedings of the Seventh Annual International Conference on Sandwich Construction. Springer, Dordrecht, pp. 3-12.

Wineman, A.S, Rajagopal, K.R., 2000. Mechanical Response of Polymers: An Introduction. Cambridge University Press, Cambridge.

Yeh, H., Kim, C.H., 1994. The mixed mode fracture analysis of unidirectional composites. Journal of Reinforced Plastics and Composites 13, 498-508.

VITA

Name: Altramese LaShé Roberts-Tompkins

Address: Texas A&M University
Department of Mechanical Engineering
c/o: Dr. Anastasia Muliana
3123 TAMU
College Station, TX 77843-3123

Email Address: robertsal2000@yahoo.com

Education: B.S., Mechanical Engineering, University of Detroit Mercy, 2003
M.S., Mechanical Engineering, Texas A&M University, 2009